CHAPTER 13
KEY EQUATIONS AND CHARTS FOR DESIGNING MECHANISMS

FOUR-BAR LINKAGES AND TYPICAL INDUSTRIAL APPLICATIONS

All mechanisms can be broken down into equivalent four-bar linkages. They can be considered to be the basic mechanism and are useful in many mechanical operations.

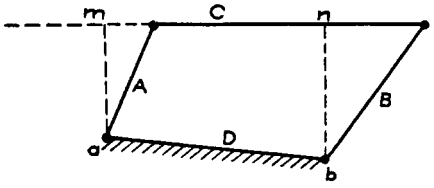

FOUR-BAR LINKAGES—Two cranks, a connecting rod and a line between the fixed centers of the cranks make up the basic four-bar linkage. Cranks can rotate if *A* is smaller than *B* or *C* or *D*. Link motion can be predicted.

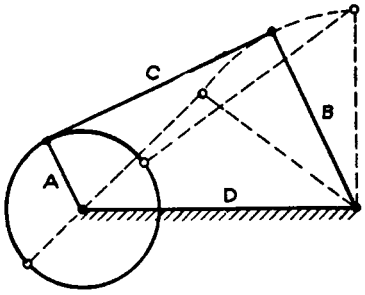

CRANK AND ROCKER—the following relations must hold for its operation: $A + B + C > D$; $A + D + B > C$; $A + C - B < D$, and $C - A + B > D$.

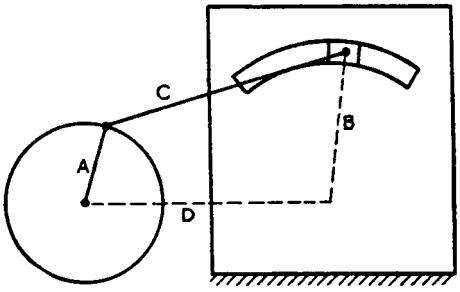

FOUR-BAR LINK WITH SLIDING MEMBER—One crank is replaced by a circular slot with an effective crank distance of *B*.

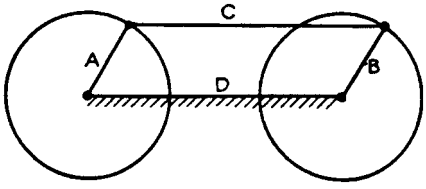

PARALLEL CRANK FOUR-BAR—Both cranks of the parallel crank four-bar linkage always turn at the same angular speed, but they have two positions where the crank cannot be effective.

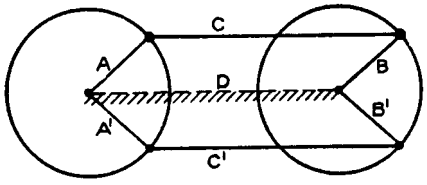

DOUBLE PARALLEL CRANK—This mechanism avoids a dead center position by having two sets of cranks at 90° advancement. The connecting rods are always parallel.

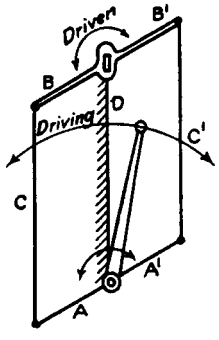

PARALLEL CRANK—Steam control linkage assures equal valve openings.

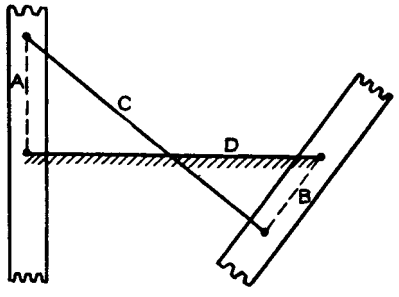

NON-PARALLEL EQUAL CRANK—The centrodes are formed as gears for passing dead center and they can replace ellipticals.

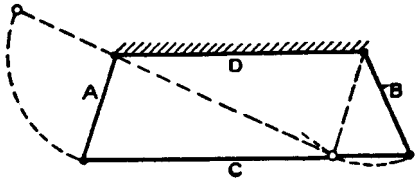

SLOW MOTION LINK—As crank *A* is rotated upward it imparts motion to crank *B*. When *A* reaches its dead center position, the angular velocity of crank *B* decreases to zero.

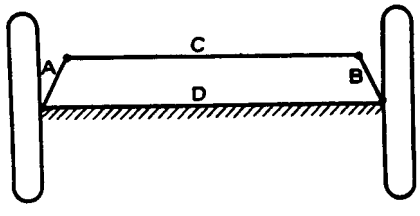

TRAPAZOIDAL LINKAGE—This linkage is not used for complete rotation but can be used for special control. The inside moves through a larger angle than the outside with normals intersecting on the extension of a rear axle in a car.

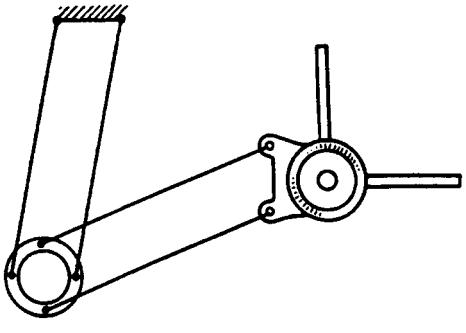

DOUBLE PARALLEL CRANK MECHANISM—This mechanism forms the basis for the universal drafting machine.

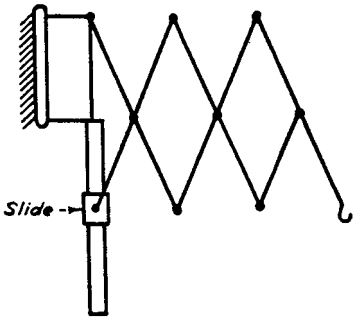

ISOSCELES DRAG LINKS—This "lazy-tong" device is made of several isosceles links; it is used as a movable lamp support.

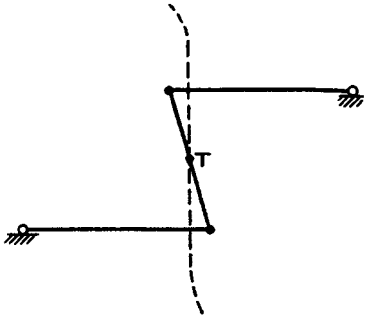

WATT'S STRAIGHT-LINE MECHANISM—Point T describes a line perpendicular to the parallel position of the cranks.

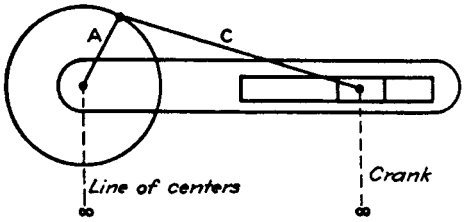

STRAIGHT SLIDING LINK—This is the form in which a slide is usually used to replace a link. The line of centers and the crank *B* are both of infinite length.

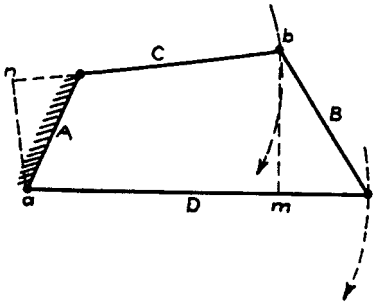

DRAG LINK—This linkage is used as the drive for slotter machines. For complete rotation: $B > A + D - C$ and $B < D + C - A$.

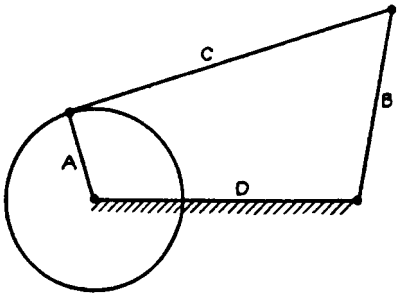

ROTATING CRANK MECHANISM—This linkage is frequently used to change a rotary motion to a swinging movement.

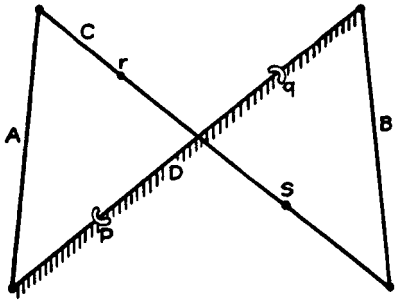

NON-PARALLEL EQUAL CRANK—If crank *A* has a uniform angular speed, *B* will vary.

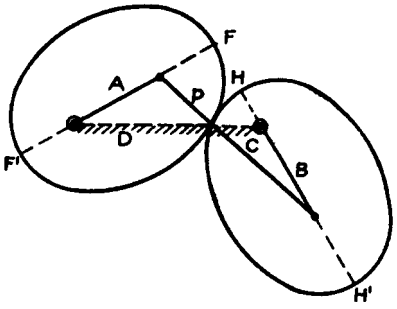

ELLIPTICAL GEARS—They produce the same motion as non-parallel equal cranks.

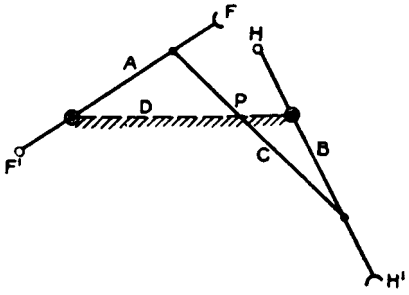

NON-PARALLEL EQUAL CRANK—It is the same as the first example given but with crossover points on its link ends.

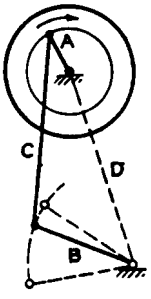

TREADLE DRIVE—This four-bar linkage is used in driving grinding wheels and sewing machines.

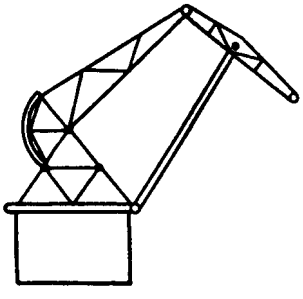

DOUBLE LEVER MECHANISM—This slewing crane can move a load in a horizontal direction by using the D-shaped portion of the top curve.

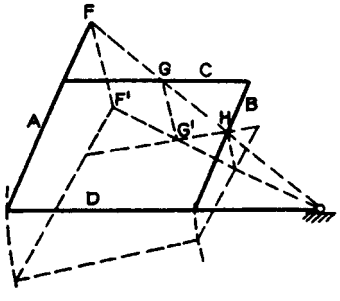

PANTOGRAPH—The pantograph is a parallelogram in which lines through *F*, *G* and *H* must always intersect at a common point.

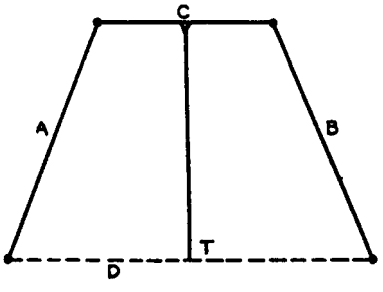

ROBERT'S STRAIGHT-LINE MECHANISM—The lengths of cranks *A* and *B* should not be less than 0.6 *D*; *C* is one half of *D*.

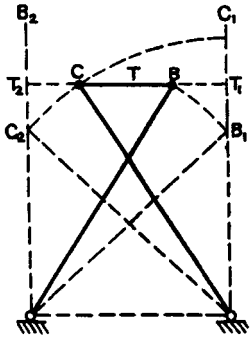

TCHEBICHEFF'S—Links are made in proportion: $AB = CD = 20$, $AD = 16$, $BC = 8$.

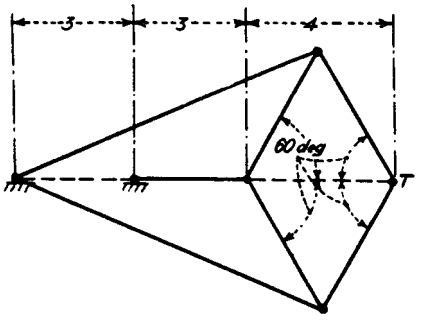

PEAUCELLIER'S CELL—When proportioned as shown, the tracing point *T* forms a straight line perpendicular to the axis.

DESIGNING GEARED FIVE-BAR MECHANISMS

Geared five-bar mechanisms offer excellent force-transmission characteristics and can produce more complex output motions—including dwells—than conventional four-bar mechanisms.

It is often necessary to design a mechanism that will convert uniform input rotational motion into nonuniform output rotation or reciprocation. Mechanisms designed for such purposes are usually based on four-bar linkages. Those linkages produce a sinusoidal output that can be modified to yield a variety of motions.

Four-bar linkages have their limitations, however. Because they cannot produce dwells of useful duration, the designer might have to include a cam when a dwell is desired, and he might have to accept the inherent speed restrictions and vibration associated with cams. A further limitation of four-bar linkages is that only a few kinds have efficient force-transmission capabilities.

One way to increase the variety of output motions of a four-bar linkage, and obtain longer dwells and better force transmissions, is to add a link. The resulting five-bar linkage would become impractical, however, because it would then have only two degrees of freedom and would, consequently, require two inputs to control the output.

Simply constraining two adjacent links would not solve the problem. The five-bar chain would then function effectively only as a four-bar linkage. If, on the other hand, any two nonadjacent links are constrained so as to remove only one degree of freedom, the five-bar chain becomes a functionally useful mechanism.

Gearing provides solution. There are several ways to constrain two nonadjacent links in a five-bar chain. Some possibilities include the use of gears, slot-and-pin joints, or nonlinear band mechanisms. Of these three possibilities, gearing is the most attractive. Some practical gearing systems (Fig. 1) included paired external gears, planet gears revolving within an external ring gear, and planet gears driving slotted cranks.

In one successful system (Fig. 1A) each of the two external gears has a fixed crank that is connected to a crossbar by a rod. The system has been successful in high-speed machines where it transforms rotary motion into high-impact linear motion. The Stirling engine includes a similar system (Fig. 1B).

In a different system (Fig. 1C) a pin on a planet gear traces an epicyclic, three-lobe curve to drive an output crank back and forth with a long dwell at the

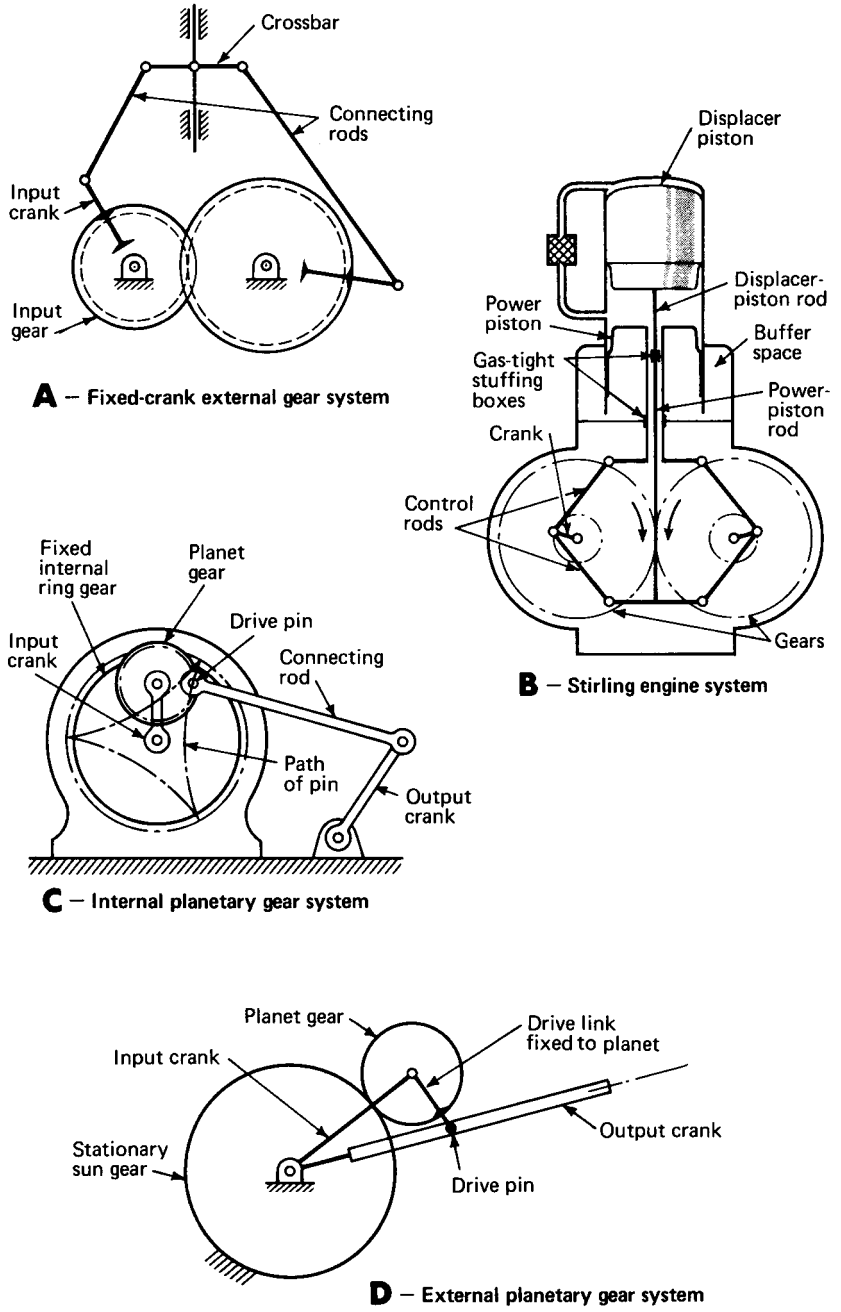

Fig. 1 Five-bar mechanism designs can be based on paired external gears or planetary gears. They convert simple input motions into complex outputs.

extreme right-hand position. A slotted output crank (Fig. 1D) will provide a similar output.

Two professors of mechanical engineering, Daniel H. Suchora of Youngstown State University, Youngstown, Ohio, and Michael Savage of the University of Akron, Akron, Ohio, studied a variation of this mechanism in detail.

Five kinematic inversions of this form (Fig. 2) were established by the two researchers. As an aid in distinguishing between the five, each type is named according to the link which acts as the fixed link. The study showed that the Type 5 mechanism would have the greatest practical value.

In the Type 5 mechanism (Fig. 3A), the gear that is stationary acts as a sun gear. The input shaft at Point E drives the input crank which, in turn, causes the planet gear to revolve around the sun gear. Link a_2, fixed to the planet, then drives the output crank, Link a_4, by means of the connecting link, Link a_3. At any input position, the third and fourth links can be assembled in either of two distinct positions or "phases" (Fig. 3B).

Variety of outputs. The different kinds of output motions that can be obtained from a Type 5 mechanism are based on the different epicyclic curves traced by link joint B. The variables that control the shape of a "B-curve" are the gear ratio GR ($GR = N_2/N_5$), the link ratio a_2/a_1 and the initial position of the gear set, defined by the initial positions of θ_1 and θ_2, designated as θ_{10} and θ_{20}, respectively.

Typical B-curve shapes (Fig. 4) include ovals, cusps, and loops. When the B-curve is oval (Fig. 4B) or semioval (Fig. 4C), the resulting B-curve is similar to the true-circle B-curve produced by a four-bar linkage. The resulting output motion of Link a_4 will be a sinusoidal type of oscillation, similar to that produced by a four-bar linkage.

When the B-curve is cusped (Fig. 4A), dwells are obtained. When the B-curve is looped (Figs. 4D and 4E), a double oscillation is obtained.

In the case of the cusped B-curve (Fig. 4A), dwells are obtained. When the B-curve is looped (Figs. 4D and 4E), a double oscillation is obtained.

In the case of the cusped B-curve (Fig. 4A), by selecting a_2 to be equal to the pitch radius of the planet gear r_2, link joint B becomes located at the pitch circle of the planet gear. The gear ratio in all the cases illustrated is unity ($GR = 1$).

Professors Suchora and Savage analyzed the different output motions produced by the geared five-bar mechanisms by plotting the angular position θ_4 of the output link a_4 of the output link a_4 against the angular position of the input link θ_1 for a variety of mechanism configurations (Fig. 5).

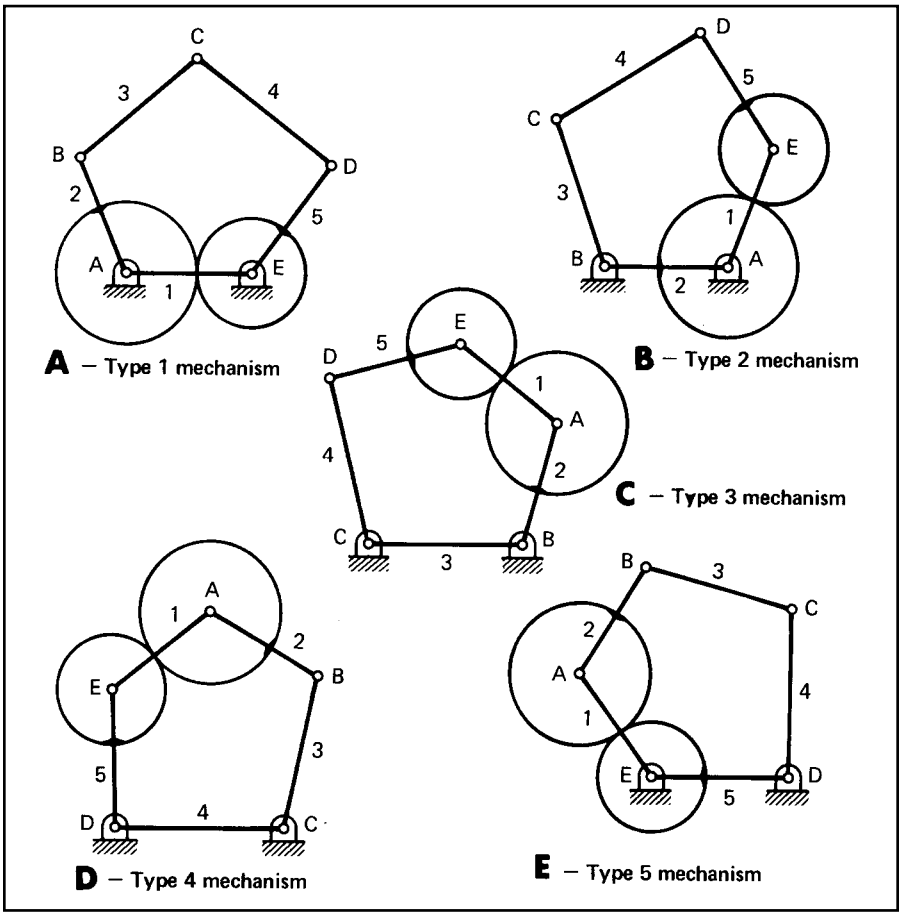

Fig. 2 Five types of geared five-bar mechanisms. A different link acts as the fixed link in each example. Type 5 might be the most useful for machine design.

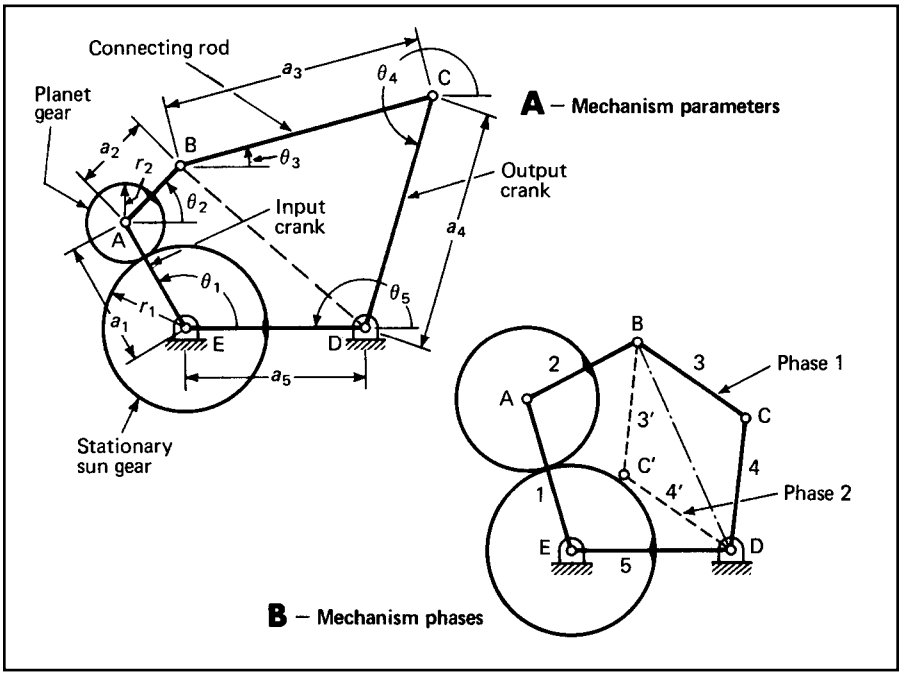

Fig. 3 A detailed design of a Type-5 mechanism. The input crank causes the planet gear to revolve around the sun gear, which is always stationary.

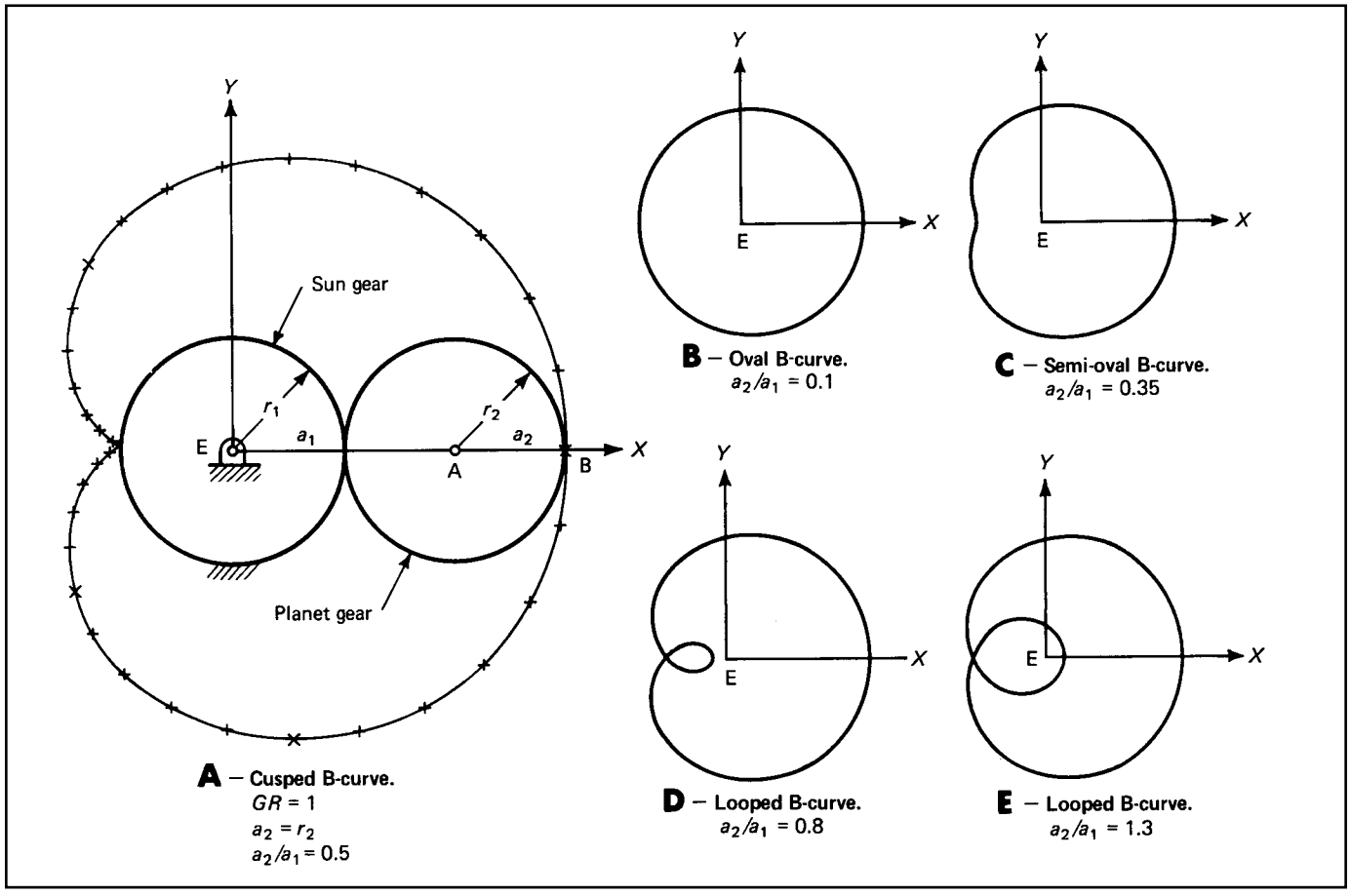

Fig. 4 Typical B-curve shapes obtained from various Type-5 geared five-bar mechanisms. The shape of the epicyclic curved is changed by the link ratio a_2/a_1 and other parameters, as described in the text.

Calculating displacement, velocity and acceleration

Displacement θ_4 can be found from the following equation:

$$\theta_4 = 2 \tan^{-1} \left(\frac{I \pm \sqrt{I^2 + H^2 - J^2}}{H + J} \right)$$

where $H = a_1 \cos \theta_1 + a_2 \cos \theta_2 - a_5$; $I = a_1 \sin \theta_1 + a_2 \sin \theta_2$; and $J = 1/2a_4 (a^2_3 - a^2_4 - H^2 - I^2)$; and where $\theta_2 = \theta_{20} + (1 + 1/GR)(\theta_1 - \theta_{10})$, where θ_{10} and θ_{20} are the initial values of the angles θ_1 and θ_2, respectively.

For layout purposes, once θ_4 is determined, θ_3 can be found from:

$$\theta_3 = \tan^{-1} \left(\frac{a_4 \sin \theta_4 + I}{a_4 \cos \theta_4 + H} \right)$$

To find velocities θ'_4 and θ'_3, use these equations:

$$\theta'_4 = \frac{a_1 \sin (\theta_3 - \theta_1) + a_2 \sin (\theta_3 - \theta_2)\, \theta'_2}{a_4 \sin (\theta_4 - \theta_3)}$$

$$\theta'_3 = \frac{a_1 \sin (\theta_1 - \theta_4) + a_2 \sin (\theta_2 - \theta_4)\, \theta'_2}{a_4 \sin (\theta_4 - \theta_3)}$$

where $\theta'_2 = (1 + 1/GR)$.

Use these equations to determine accelerations θ''_4 and θ''_3:

$$\theta''_4 = \frac{L}{a_3\, a_4 \sin (\theta_4 - \theta_3)}$$

$$\theta''_3 = \frac{K}{a_3\, a_4 \sin (\theta_4 - \theta_3)}$$

where $K = a_3 a_4 \cos(\theta_3 - \theta_4)\, \theta'^2_3 + a_4^2 \theta'^2_4 + a_1 a_2 \cos(\theta_1 - \theta_4) + a_2 a_4 \cos(\theta_2 - \theta_4) \theta'^2_2$ and $L = a_3^2 \theta'^2_3 - a_3 a_1 \cos(\theta_3 - \theta_4) \theta'^2_4 - a_1 a_3 \cos(\theta_3 - \theta_1) + a_2 a_3 \cos(\theta_3 - \theta_2) \theta'^2_2$.

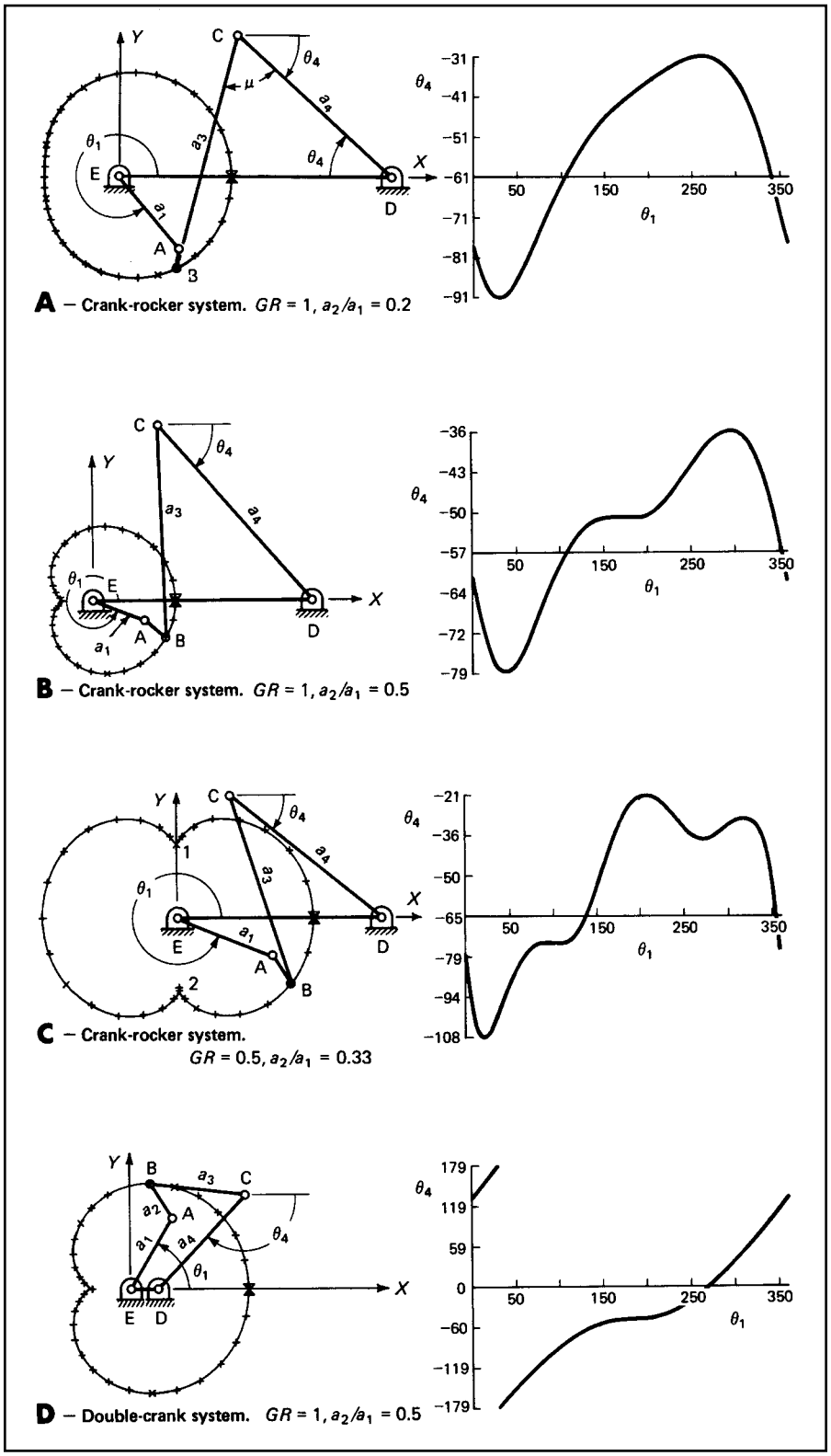

Fig. 5 A variety of output motions can be produced by varying the design of five-bar geared mechanisms. Dwells are obtainable with proper design. Force transmission is excellent. In these diagrams, the angular position of the output link is plotted against the angular position of the input link for various five-bar mechanism designs.

In three of the four cases illustrated, $GR = 1$, although the gear pairs are not shown. Thus, one input rotation generates the entire path of the B-curve. Each mechanism configuration produces a different output.

One configuration (Fig. 5A) produces an approximately sinusoidal reciprocating output motion that typically has better force-transmission capabilities than equivalent four-bar outputs. The transmission angle μ should be within 45 to 135° during the entire rotation for best results.

Another configuration (Fig. 5B) produces a horizontal or almost-horizontal portion of the output curve. The output link, link, a_4, is virtually stationary during this period of input rotation—from about 150 to 200° of input rotation θ_1 in the case illustrated. Dwells of longer duration can be designed.

By changing the gear ratio to 0.5 (Fig. 5C), a complex motion is obtained; two intermediate dwells occur at cusps 1 and 2 in the path of the B-curve. One dwell, from $\theta_1 = 80$ to 110°, is of good quality. The dwell from 240 to 330° is actually a small oscillation.

Dwell quality is affected by the location of Point D with respect to the cusp, and by the lengths of links a_3 and a_4. It is possible to design this form of mechanism so it will produce two usable dwells per rotation of input.

In a double-crank version of the geared five-bar mechanism (Fig. 5D), the output link makes full rotations. The output motion is approximately linear, with a usable intermediate dwell caused by the cusp in the path of the B-curve.

From this discussion, it's apparent that the Type 5 geared mechanism with $GR = 1$ offers many useful motions for machine designers. Professors Suchora and Savage have derived the necessary displacement, velocity, and acceleration equations (see the "Calculating displacement, velocity, and acceleration" box).

KINEMATICS OF INTERMITTENT MECHANISMS— THE EXTERNAL GENEVA WHEEL

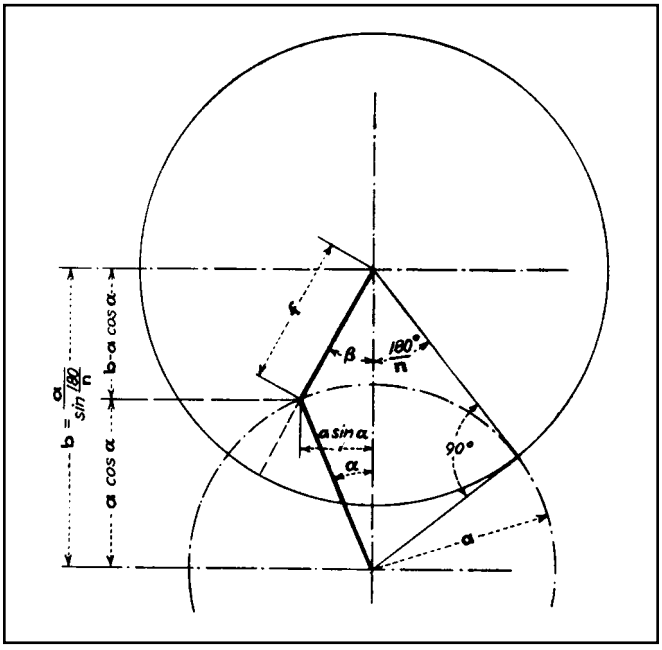

Fig. 1 A basic outline drawing for the external geneva wheel. The symbols are identified for application in the basic equations.

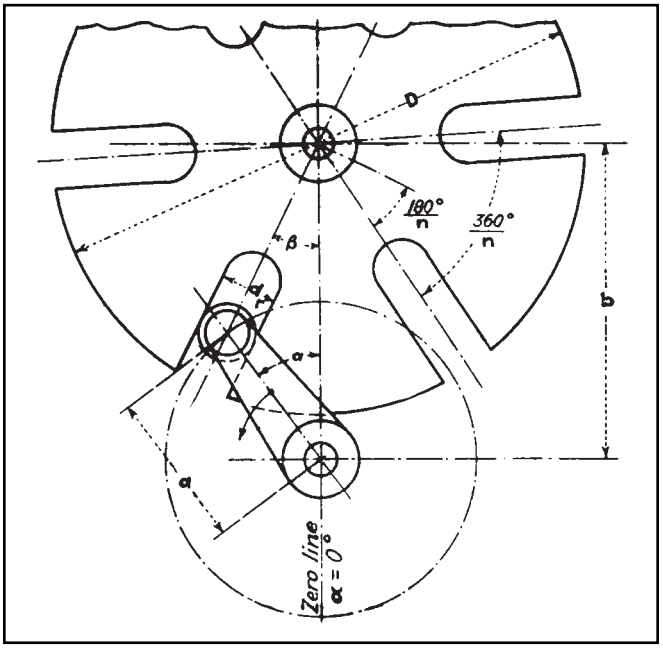

Fig. 2 A schematic drawing of a six-slot geneva wheel. Roller diameter, d_r, must be considered when determining D.

Table I—Notation and Formulas for the External Geneva Wheel

Assumed or given: a, n, d and p

a = crank radius of driving member
n = number of slots
d_r = roller diameter
p = constant velocity of driving crank in rpm

$$m = \frac{1}{\sin \frac{180}{n}}$$

b = center distance = am

$$D = \text{diameter of driven member} = 2\sqrt{\frac{d_r^2}{4} + a^2 \cot^2 \frac{180}{n}}$$

$$\omega = \text{constant angular velocity of driving crank} = \frac{p\pi}{30} \text{ radians per sec}$$

α = angular position of driving crank at any time

β = angular displacement of driven member corresponding to crank angle α

$$\cos\beta = \frac{m - \cos\alpha}{\sqrt{1 + m^2 - 2m\cos\alpha}}$$

$$\text{Angular Velocity of driven member} = \frac{d\beta}{dt} = \omega\left(\frac{m\cos\alpha - 1}{1 + m^2 - 2m\cos\alpha}\right)$$

$$\text{Angular Acceleration of driven member} = \frac{d^2\beta}{dt^2} = \omega^2\left(\frac{m\sin\alpha\,(1 - m^2)}{(1 + m^2 - 2m\cos\alpha)^2}\right)$$

Maximum Angular Acceleration occurs when $\cos\alpha =$

$$\sqrt{\left(\frac{1 + m^2}{4m}\right)^2 + 2} - \left(\frac{1 + m^2}{4m}\right)$$

Maximum Angular Velocity occurs at $\alpha = 0$ deg, and equals

$$\frac{\omega}{m - 1} \text{ radians per sec}$$

One of the most commonly applied mechanisms for producing intermittent rotary motion from a uniform input speed is the external geneva wheel.

The driven member, or star wheel, contains many slots into which the roller of the driving crank fits. The number of slots determines the ratio between dwell and motion period of the driven shaft. The lowest possible number of slots is three, while the highest number is theoretically unlimited. In practice, the three-slot geneva is seldom used because of the extremely high acceleration values encountered. Genevas with more than 18 slots are also infrequently used because they require wheels with comparatively large diameters.

In external genevas of any number of slots, the dwell period always exceeds the motion period. The opposite is true of the internal geneva. However, for the spherical geneva, both dwell and motion periods are 180°.

For the proper operation of the external geneva, the roller must enter the slot tangentially. In other words, the centerline of the slot and the line connecting the roller center and crank rotation center must form a right angle when the roller enters or leaves the slot.

The calculations given here are based on the conditions stated here.

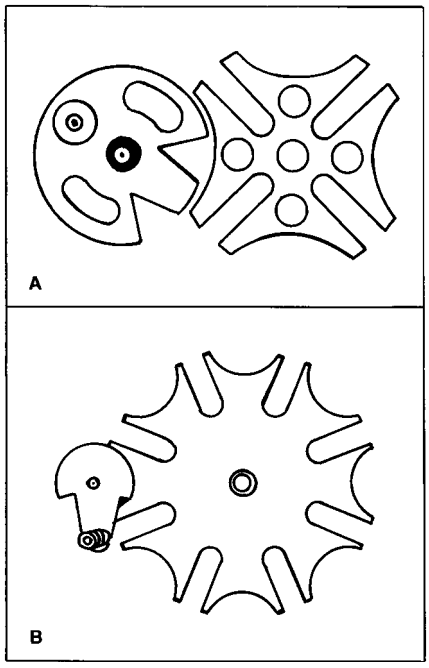

Fig. 3 A four-slot geneva (A) and an eight-slot geneva (B). Both have locking devices.

Consider an external geneva wheel, shown in Fig. 1, in which

n = number of slots

a = crank radius

From

$$\text{Fig. 1, } b = \text{center distance} = \frac{a}{\sin\frac{180}{n}}$$

$$\text{Let } \frac{1}{\sin\frac{180}{n}} = m$$

Then $b = am$

It will simplify the development of the equations of motion to designate the connecting line of the wheel and crank centers as the zero line. This is contrary to the practice of assigning the zero value of α, representing the angular position of the driving crank, to that position of the crank where the roller enters the slot.

Thus, from Fig. 1, the driven crank radius f at any angle is:

$$f = \sqrt{(am - a\cos\alpha)^2 + \alpha^2\sin^2\alpha}$$

$$= \alpha\sqrt{1 + m^2 - 2m\cos\alpha} \qquad (1)$$

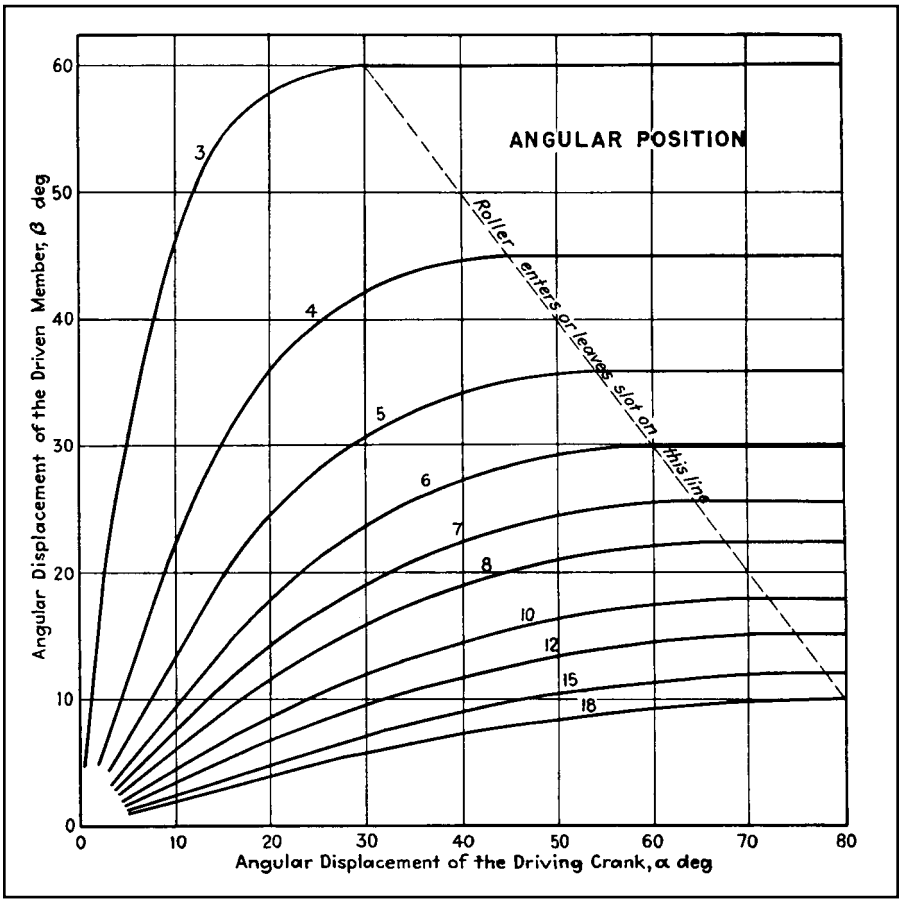

Fig. 4 Chart for determining the angular displacement of the driven member.

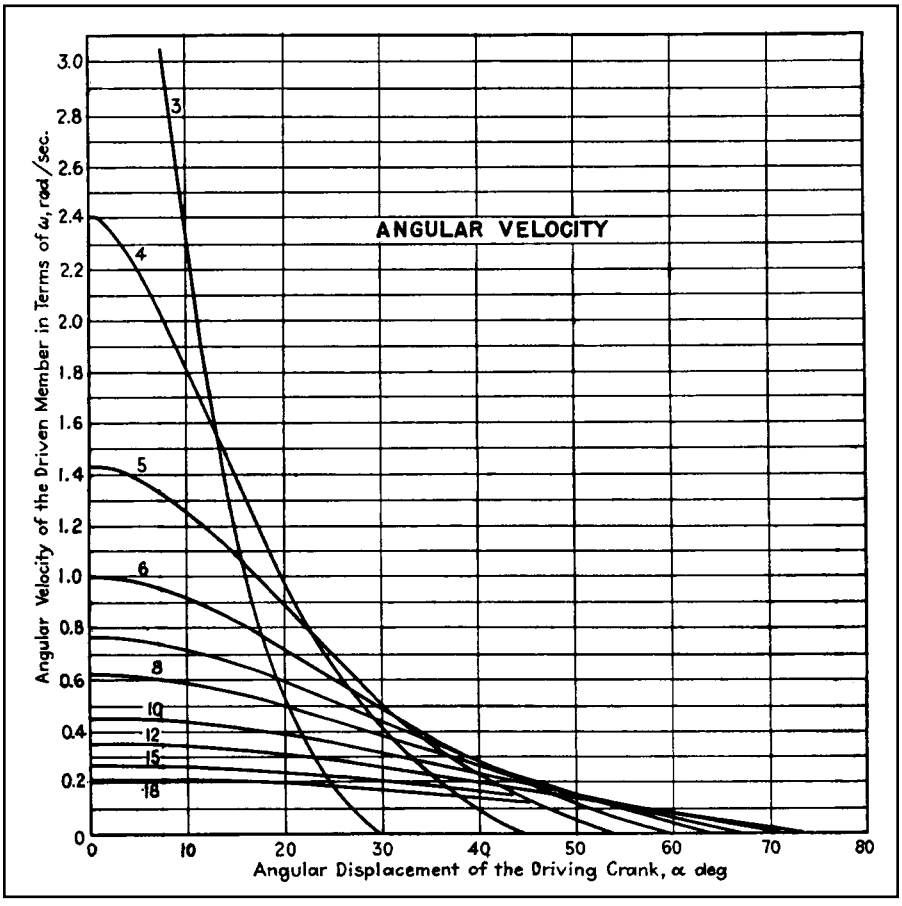

Fig. 5 Chart for determining the angular velocity of the driven member.

Table II—Principal Kinematic Data for External Geneva Wheel

No. of Slots	$\frac{360°}{n}$	Dwell period	Motion period	m and center-distance for $\alpha = 1$	Maximum angular velocity of driven member, radians per sec. equals ω multiplied by values tabulated. Crank at 0° position	Angular acceleration of driven member when roller enters slot, radians² per sec², equals ω^2 multiplied by values tabulated.			Maximum angular Acceleration of driven member, radians² per sec², equals ω^2 multiplied by values tabulated		
						α	β	Multiplier	α	β	Multiplier
3	120°	300°	60°	1.155	6.458	30°	60°	1.729	4°	27° 58′	29.10
4	90°	270°	90°	1.414	2.407	45°	45°	1.000	11° 28′	25° 11′	5.314
5	72°	252°	108°	1.701	1.425	54°	36°	0.727	17° 31′	21° 53′	2.310
6	60°	240°	120°	2.000	1.000	60°	30°	0.577	22° 55′	19° 51′	1.349
7	51° 25′ 43″	231° 30′	128° 30′	2.305	0.766	64° 17′ 8″	25° 42′ 52″	0.481	27° 41′	18° 11′	0.928
8	45°	225°	135°	2.613	0.620	67° 30′	22° 30′	0.414	31° 38′	16° 32′	0.700
9	40°	220°	140°	2.924	0.520	70°	20°	0.364	35° 16′	15° 15′	0.559
10	36°	216°	144°	3.236	0.447	72°	18°	0.325	38° 30′	14° 16′	0.465
11	32° 43′ 38″	212° 45′	147° 15′	3.549	0.392	73° 38′ 11″	16° 21′ 49″	0.294	41° 22′	13° 16′	0.398
12	30°	210°	150°	3.864	0.349	75°	15°	0.268	44°	12° 26′	0.348
13	27° 41′ 32″	207° 45′	152° 15′	4.179	0.315	76° 9′ 14″	13° 50′ 46″	0.246	46° 23′	11° 44′	0.309
14	25° 42′ 52″	205° 45′	154° 15′	4.494	0.286	77° 8′ 34″	21° 51′ 26″	0.228	48° 32′	11° 3′	0.278
15	24°	204°	156°	4.810	0.263	78°	12°	0.213	50° 30′	10° 27′	0.253
16	22° 30′	202° 30′	157° 30′	5.126	0.242	78° 45′	11° 15′	0.199	52° 24′	9° 57′	0.232
17	21°10′ 35″	201°	159°	5.442	0.225	79° 24′ 43″	10° 35′ 17″	0.187	53° 58′	9° 26′	0.215
18	20°	200°	160°	5.759	0.210	80°	10°	0.176	55° 30′	8° 59′	0.200

and the angular displacement β can be found from:

$$\cos\beta = \frac{m - \cos a}{\sqrt{1 + m^2 - 2m\cos\alpha}} \qquad (2)$$

A six-slot geneva is shown schematically in Fig. 2. The outside diameter D of the wheel (when accounting for the effect of the roller diameter d) is found to be:

$$D = 2\sqrt{\frac{d_r^2}{4} + a^2 \cot^2 \frac{180}{n}} \qquad (3)$$

Differentiating Eq. (2) and dividing by the differential of time, dt, the angular velocity of the driven member is:

$$\frac{d\beta}{dt} = \omega\left(\frac{m\cos\alpha - 1}{1 + m^2 - 2m\cos\alpha}\right) \qquad (4)$$

where ω represents the constant angular velocity of the crank.

By differentiation of Eq. (4) the acceleration of the driven member is found to be:

$$\frac{d^2\beta}{dt^2} = \omega^2\left(\frac{m\sin\alpha(1 - m^2)}{(1 + m^2 - 2m\cos\alpha)^2}\right) \qquad (5)$$

All notations and principal formulas are given in Table I for easy reference. Table II contains all the data of principal interest for external geneva wheels having from 3 to 18 slots. All other data can be read from the charts: Fig. 4 for angular position, Fig. 5 for angular velocity, and Fig. 6 for angular acceleration.

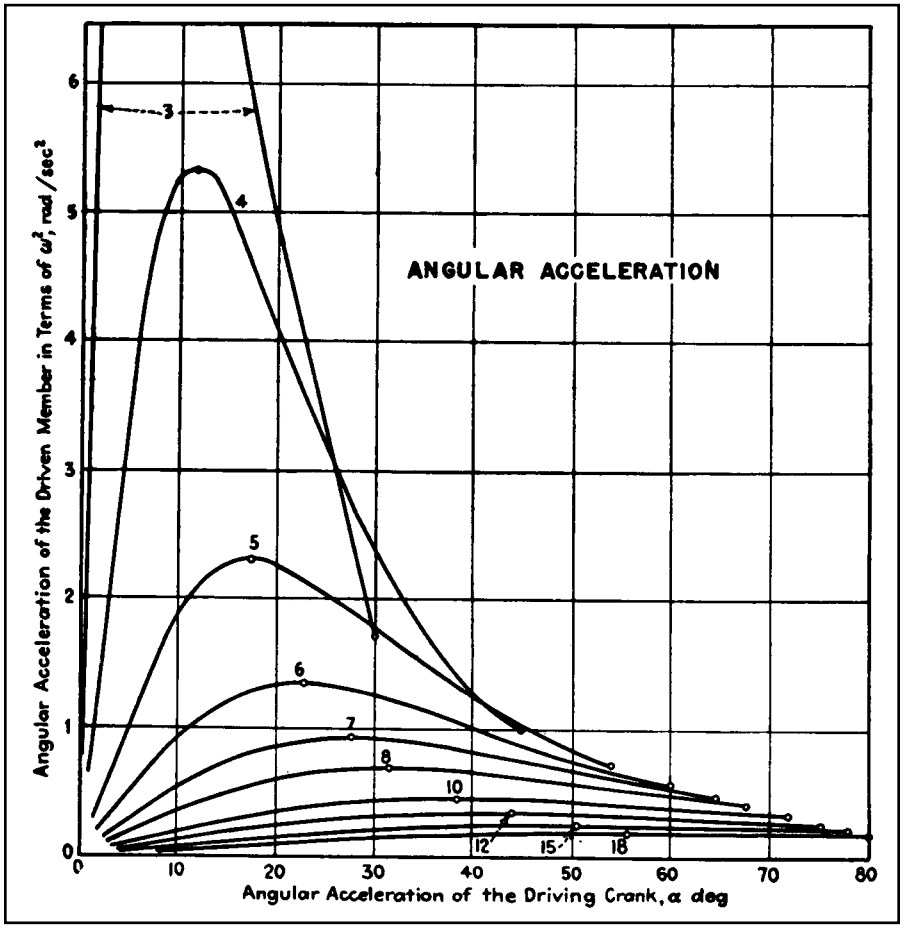

Fig. 6 Chart for determining the angular acceleration of the driven member.

KINEMATICS OF INTERMITTENT MECHANISMS— THE INTERNAL GENEVA WHEEL

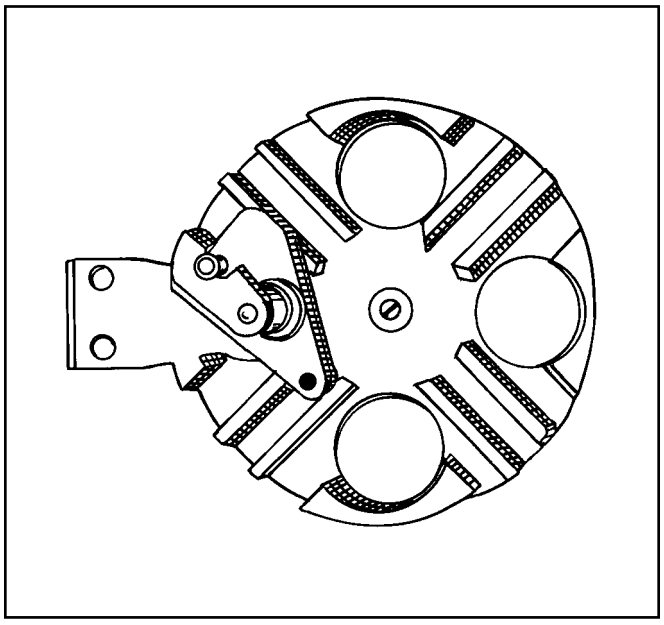

Fig. 1 A four-slot internal geneva wheel incorporating a locking mechanism. The basic sketch is shown in Fig. 3.

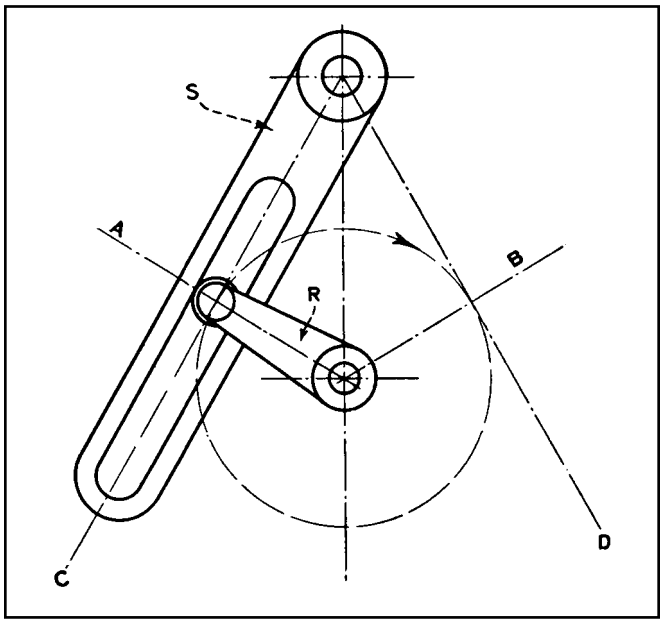

Fig. 2 Slot-crank motion from *A* to *B* represents external geneva action; from *B* to *A* represents internal geneva motion.

Where intermittent drives must provide dwell periods of more than 180°, the external geneva wheel design is satisfactory and is generally the standard device employed. But where the dwell period must be less than 180°, other intermittent drive mechanisms must be used. The internal geneva wheel is one way of obtaining this kind of motion.

The dwell period of all internal genevas is always smaller than 180°. Thus, more time is left for the star wheel to reach maximum velocity, and acceleration is lower. The highest value of angular acceleration occurs when the roller enters or leaves the slot. However, the acceleration occurs when the roller enters or leaves the slot. However, the acceleration curve does not reach a peak within the range of motion of the driven wheel. The geometrical maximum would occur in the continuation of the curve. But this continuation has no significance because the driven member will have entered the dwell phase associated with the high angular displacement of the driving member.

The geometrical maximum lies in the continuation of the curve, falling into the region representing the motion of the external geneva wheel. This can be seen by the following considerations of a crank and slot drive, drawn in Fig. 2.

When the roller crank *R* rotates, slot link *S* will perform an oscillating move-

Table I—Notation and Formulas for the Internal Geneva Wheel

Assumed or given: a, n, d and p

a = crank radius of driving member
n = number of slots
d = roller diameter
p = constant velocity of driving crank in rpm

$$m = \frac{1}{\sin \frac{180^\circ}{n}}$$

b = center distance = $a\,m$

$$D = \text{inside diameter of driven member} = 2\sqrt{\frac{d^2}{4} + a^2 \cot^2 \frac{180^\circ}{n}}$$

ω = constant angular velocity of driving crank in radians per sec = $\frac{p\pi}{30}$ radians per sec

α = angular position of driving crank at any time
β = angular displacement of driven member corresponding to crank angle α

$$\cos\beta = \frac{m + \cos\alpha}{\sqrt{1 + m^2 + 2m\cos\alpha}}$$

$$\text{Angular velocity of driven member} = \frac{d\beta}{dt} = \omega\left(\frac{1 + m\cos\alpha}{1 + m^2 + 2m\cos\alpha}\right)$$

$$\text{Angular acceleration of driven member} = \frac{d^2\beta}{dt^2} = \omega^2\left[\frac{m\sin\alpha\,(1 - m^2)}{(1 + m^2 + 2m\cos\alpha)^2}\right]$$

Maximum angular velocity occurs at $\alpha = 0°$ and equals = $\frac{\omega}{1 + m}$ radians per sec

Maximum angular acceleration occurs when roller enters slot and equals = $\frac{\omega^2}{\sqrt{m^2 - 1}}$ radians^2 per sec^2

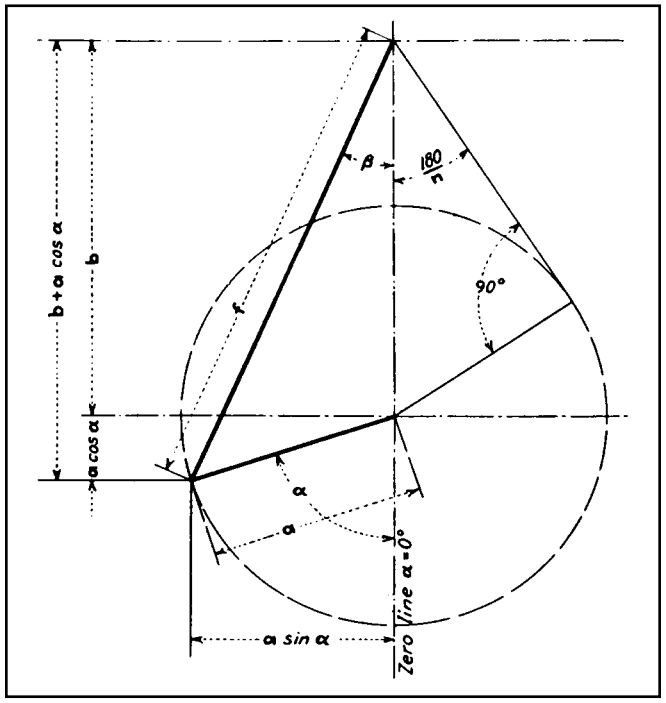

Fig. 3 A basic outline for developing the equations of the internal geneva wheel, based on the notations shown.

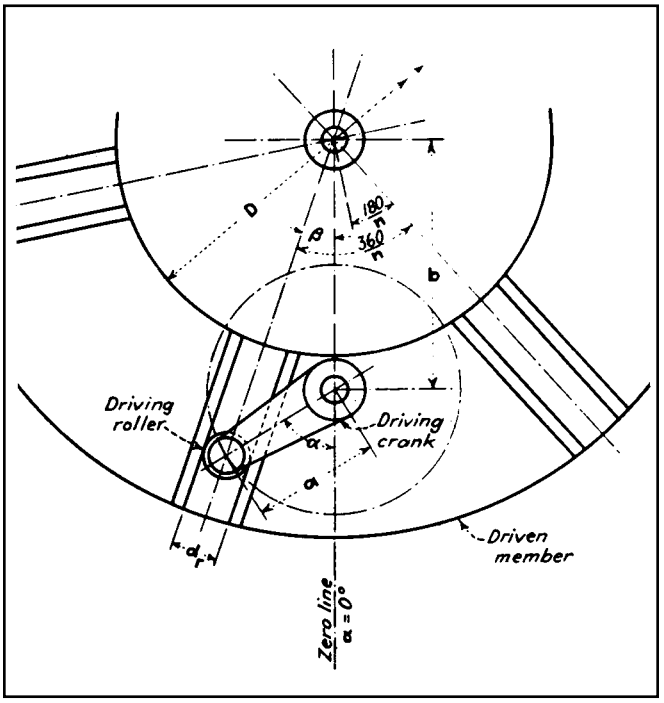

Fig. 4 A drawing of a six-slot internal geneva wheel. The symbols are identified, and the motion equations are given in Table I.

ment, for which the displacement, angular velocity, and acceleration can be given in continuous curves.

When the crank *R* rotates from *A* to *B*, then the slot link *S* will move from *C* to *D*, exactly reproducing all moving conditions of an external geneva of equal slot angle. When crank *R* continues its movement from *B* back to *A*, then the slot link *S* will move from *D* back to *C*, this time reproducing exactly (though in a mirror picture with the direction of motion being reversed) the moving conditions of an internal geneva.

Therefore, the characteristic curves of this motion contain both the external and internal geneva wheel conditions; the region of the external geneva lies between *A* and *B*, the region of the internal geneva lies between *B* and *A*.

The geometrical maxima of the acceleration curves lie only in the region between *A* and *B*, representing that portion of the curves which belongs to the external geneva.

The principal advantage of the internal geneva, other than its smooth operation, is it sharply defined dwell period. A disadvantage is the relatively large size of the driven member, which increases the force resisting acceleration. Another feature, which is sometimes a disadvantage, is the cantilever arrangement of the roller crank shaft. This shaft cannot be a through shaft because the crank must be fastened to the overhanging end of the input shaft.

To simplify the equations, the connecting line of the wheel and crank centers is taken as the zero line. The angular

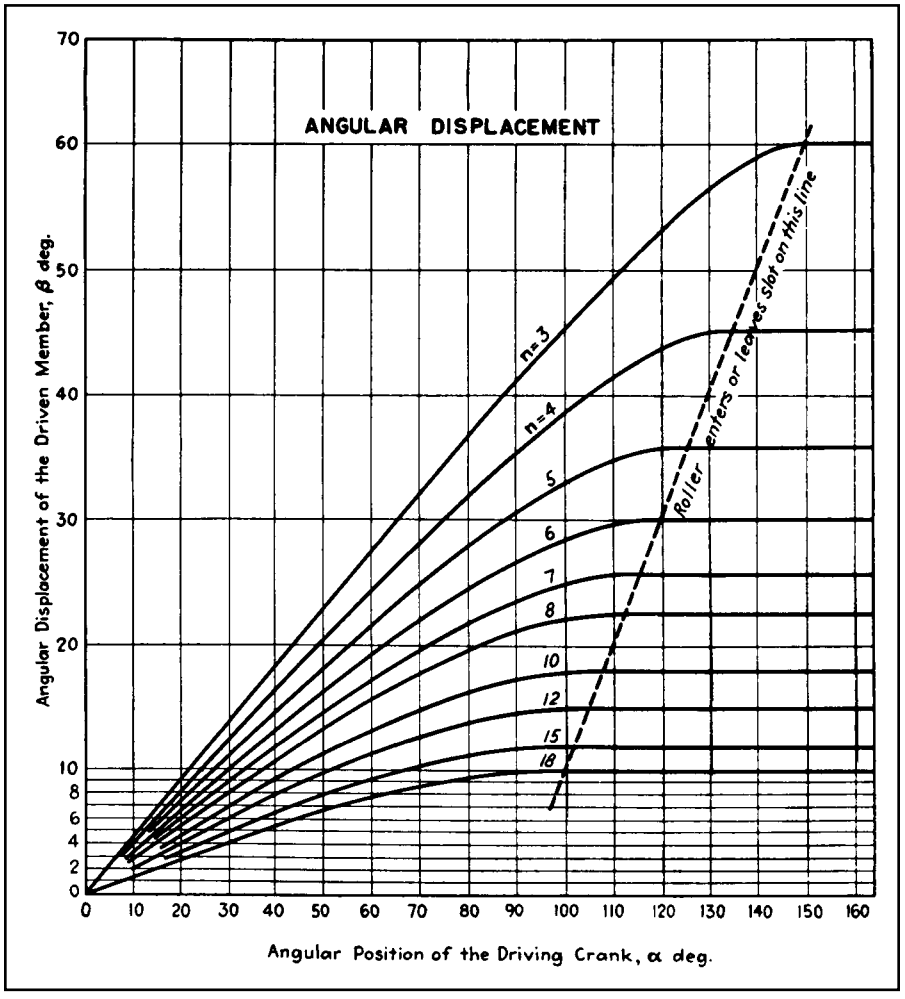

Fig. 5 Angular displacement of the driven member can be determined from this chart.

position of the driving crank α is zero when it is on this line. Then the following relations are developed, based on Fig. 3.

n = number of slots
a = crank radius
b = center distance = $\dfrac{a}{\sin\dfrac{180^\circ}{n}}$

Let

$$\frac{1}{\sin\dfrac{180^\circ}{n}} = m,$$

then; $b = am$

To find the angular displacement β of the driven member, the driven crank radius f is first calculated from:

$$f = \sqrt{a^2\sin^2\alpha + (am + a\cos\alpha)^2}$$
$$= \alpha\sqrt{1 + m^2 + 2m\cos\alpha} \qquad (1)$$

and because

$$\cos\beta = \frac{m + \cos\alpha}{f}$$

it follows:

$$\cos\beta = \frac{m + \cos\alpha}{\sqrt{1 + m^2 + 2m\cos\alpha}} \qquad (2)$$

From this formula, β, the angular displacement, can be calculated for any angle α, the angle of the mechanism's driving member.

The first derivative of Eq. (2) gives the angular velocity as:

$$\frac{d\beta}{dt} = \omega\left(\frac{1 + m\cos\alpha}{1 + m^2 + 2m\cos\alpha}\right) \qquad (3)$$

where ω designates the uniform speed of the driving crank shaft, namely:

$$\omega = \frac{p\pi}{30}$$

if p equals its number of revolutions per minute.

Differentiating Eq. (3) once more develops the equation for the angular acceleration:

$$\frac{d^2\beta}{dt^2} = \omega^2\left[\frac{m\sin\alpha(1 - m^2)}{(1 + m^2 + 2m\cos\alpha)^2}\right] \qquad (4)$$

The maximum angular velocity occurs, obviously, at $\alpha = 0^\circ$. Its value is found by substituting 0° for α in Eq. (3). It is:

$$\frac{d\beta}{dt_{\max}} = \frac{\omega}{1 + m} \qquad (5)$$

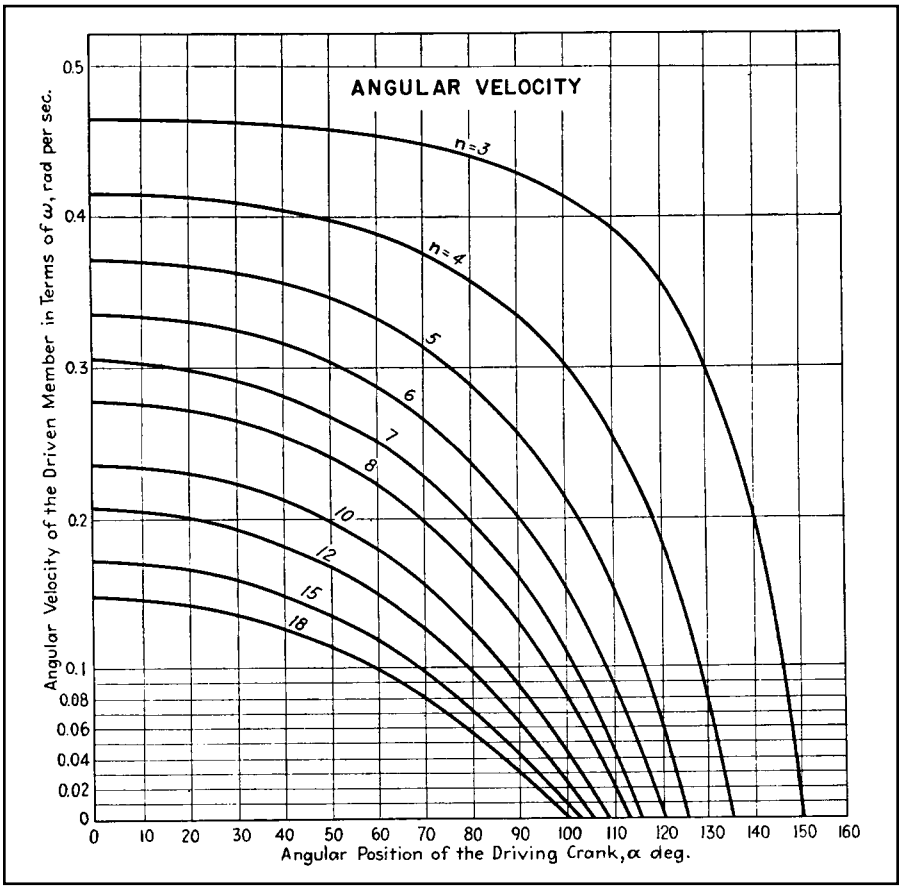

Fig. 6 Angular velocity of the driven member can be determined from this chart.

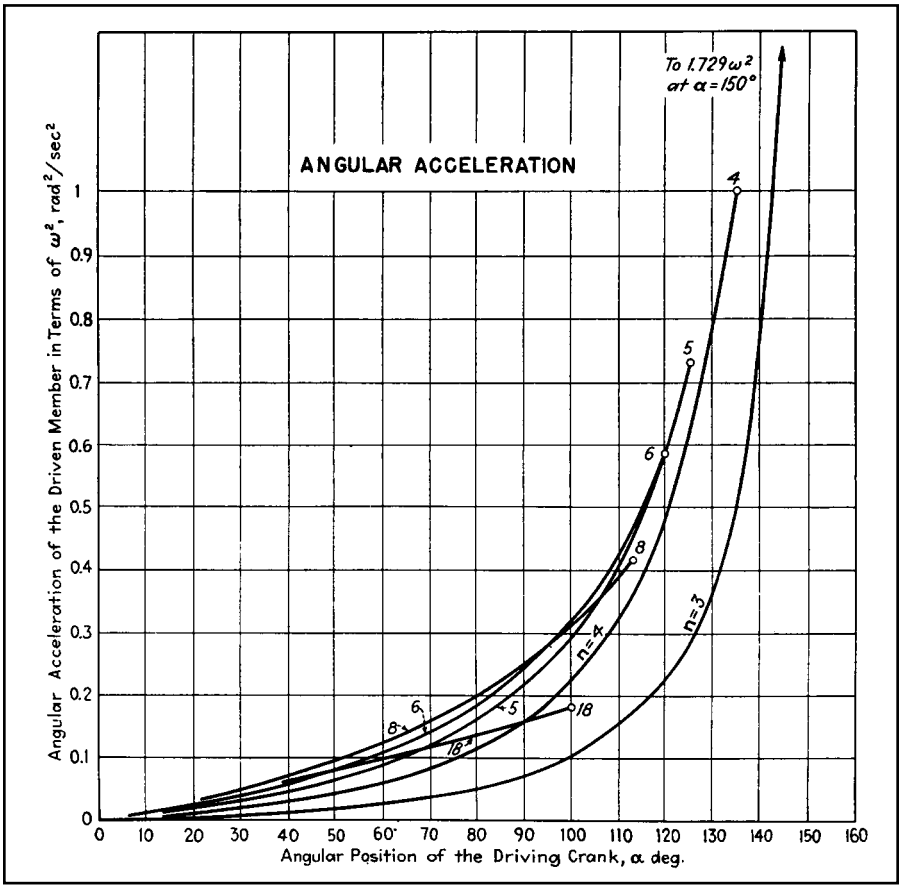

Fig. 7 Angular acceleration of the driven member can be determined from this chart.

Table II—Kinematic Data For the Internal Geneva Wheel

Number of slots, n	$\frac{360°}{n}$	Dwell period	Motion period	m and center-distance for $a=1$	Maximum angular velocity of driven member equals ω radians per sec. multiplied by values tabulated. Both α and β in 0° position	Angular acceleration of driven member when roller enters slot equals ω^2 radians² per sec² multiplied by values tabulated		
						α	β	Multiplier
3	120°	60°	300°	1.155	0.464	150°	60°	1.729
4	90°	90°	270°	1.414	0.414	135°	45°	1.000
5	72°	108°	252°	1.701	0.370	126°	36°	0.727
6	60°	120°	240°	2.000	0.333	120°	30°	0.577
7	51° 25′ 43″	128° 30′	231° 30′	2.305	0.303	115° 42′ 52″	25° 42′ 52″	0.481
8	45°	135°	225°	2.613	0.277	112° 30′	22° 30′	0.414
9	40°	140°	220°	2.924	0.255	110°	20°	0.364
10	36°	144°	216°	3.236	0.236	108°	18°	0.325
11	32° 43′ 38″	147° 15′	212° 45′	3.549	0.220	106° 21′ 49″	16° 21′ 49″	0.294
12	30°	150°	210°	3.864	0.206	105°	15°	0.268

The highest value of the acceleration is found by substituting $180/n + 980$ for α in Eq. (4):

$$\frac{d^2\beta}{dt^2_{max}} = \frac{\omega^2}{\sqrt{m^2-1}} \qquad (6)$$

A layout drawing for a six-slot internal geneva wheel is shown in Fig. 4. All the symbols in this drawing and throughout the text are compiled in Table I for easy reference.

Table II contains all the data of principal interest on the performance of internal geneva wheels that have from 3 to 18 slots. Other data can be read from the charts: Fig. 5 for angular position, Fig. 6 for angular velocity, and Fig. 7 for angular acceleration.

EQUATIONS FOR DESIGNING CYCLOID MECHANISMS

Fig. 1 Equations for epicycloid drives.

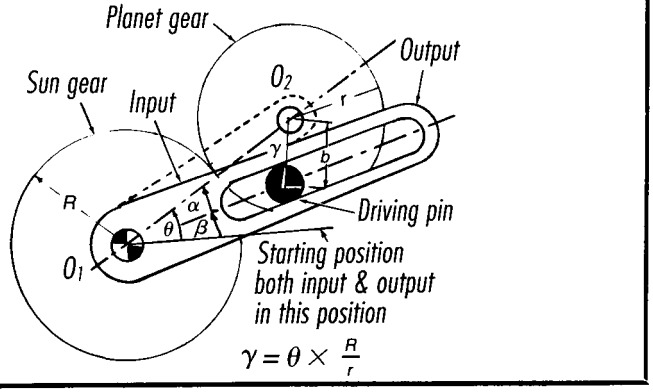

The equations for angular displacement, velocity, and acceleration for a basic epicyclic drive are given below.

Angular displacement

$$\tan\beta = \frac{(R+r)\sin\theta - b\sin(\theta+\gamma)}{(R+r)\cos\theta - b\cos(\theta+\gamma)} \qquad (1)$$

Angular velocity

$$V = \omega \frac{1+\frac{b^2}{r(R+r)} - \left(\frac{2r+R}{r}\right)\left(\frac{b}{R+r}\right)\left(\cos\frac{R}{r}\theta\right)}{1+\left(\frac{b}{R+r}\right)^2 - \left(\frac{2b}{R+r}\right)\left(\cos\frac{R}{r}\theta\right)} \qquad (2)$$

Angular acceleration

$$A = \omega^2 \frac{\left(1-\frac{b^2}{(R+r)^2}\right)\left(\frac{R^2}{r^2}\right)\left(\frac{b}{R+r}\right)\left(\sin\frac{R}{r}\theta\right)}{\left[1+\frac{b^2}{(R+r)^2} - \left(\frac{2b}{R+r}\right)\left(\cos\frac{R}{r}\theta\right)\right]^2} \qquad (3)$$

Symbols

- A = angular acceleration of output, degrees per second²
- b = radius of driving pin from center of planet gear
- r = pitch radius of planet gear
- R = pitch radius of fixed sun gear
- V = angular velocity of output, degrees per second
- β = angular displacement of output, degree
- γ = $\theta R/r$
- θ = input displacement, degree
- ω = angular velocity of input, degrees per second

Fig. 2 Equations for hypocycloid drives.

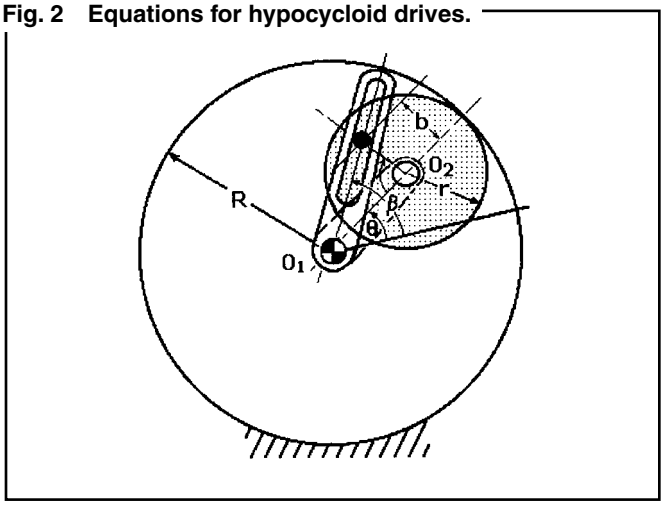

$$\tan\beta = \frac{\sin\theta - \left(\frac{b}{R-r}\right)\left(\sin\frac{R-r}{r}\theta\right)}{\cos\theta + \left(\frac{b}{R-r}\right)\left(\cos\frac{R-r}{r}\theta\right)} \tag{4}$$

$$V = \omega \frac{1 - \left(\frac{R-r}{r}\right)\left(\frac{b^2}{(R-r)^2}\right) + \left(\frac{2r-R}{r}\right)\left(\frac{b}{R-r}\right)\left(\cos\frac{R}{r}\theta\right)}{1 + \frac{b^2}{(R-r)^2} + \left(\frac{2b}{R-r}\right)\left(\cos\frac{R}{r}\theta\right)} \tag{5}$$

$$A = \omega^2 \frac{\left(1 - \frac{b^2}{(R-r)^2}\right)\left(\frac{b}{R-r}\right)\left(\frac{R^2}{r^2}\right)\left(\sin\frac{R}{r}\theta\right)}{\left[1 + \frac{b^2}{(R-r)^2} + \left(\frac{2b}{R-r}\right)\left(\cos\frac{R}{r}\theta\right)\right]^2} \tag{6}$$

DESCRIBING APPROXIMATE STRAIGHT LINES

Fig. 3 A gear rolling on a gear flattens curves.

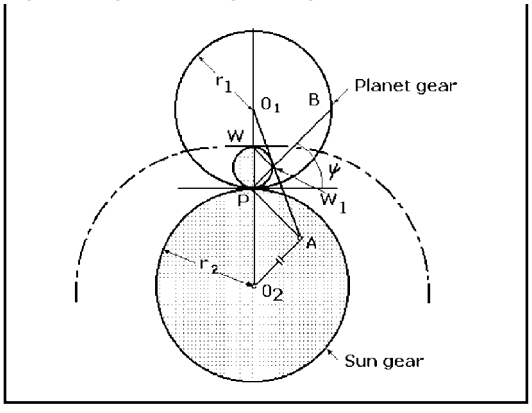

It is frequently desirable to find points on the planet gear that will describe approximately straight lines for portions of the output curves. These points will yield dwell mechanisms. Construction is as follows (see drawing):

1. Draw an arbitrary line *PB*.
2. Draw its parallel O_2A.
3. Draw its perpendicular *PA* at *P*. Locate point *A*.
4. Draw O_1A. Locate W_1.
5. Draw perpendicular to PW_1 at W_1 to locate *W*.
6. Draw a circular with *PW* as the diameter.

All points on this circle describe curves with portions that are approximately straight. This circle is also called the **inflection circle** because all points describe curves that have a point of inflection at the position illustrated. (The curve passing through point *W* is shown.)

Fig. 5 A gear rolling inside a gear describes a zig-zag.

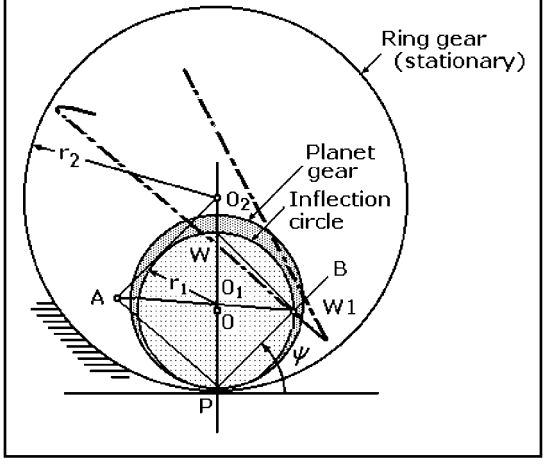

Fig. 4 A gear rolling on a rack describes vee curves.

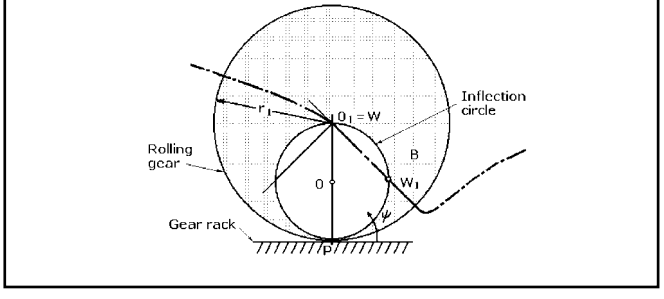

This is a special case. Draw a circle with a diameter half that of the gear (diameter O_1P). This is the inflection circle. Any point, such as point W_1, will describe a curve that is almost straight in the vicinity selected. Tangents to the curves will always pass through the center of the gear, O_1 (as shown).

To find the inflection circle for a gear rolling inside a gear:

1. Draw arbitrary line *PB* from the contact point *P*.
2. Draw its parallel O_2A, and its perpendicular, *PA*. Locate *A*.
3. Draw line AO_1 through the center of the rolling gear. Locate W_1.
4. Draw a perpendicular through W_1. Obtain *W*. Line *WP* is the diameter of the inflection circle. Point W_1, which is an arbitrary point on the circle, will trace a curve of repeated almost-straight lines, as shown.

DESIGNING FOR DWELLS

Fig. 6 The center of curvature: a gear rolling on gear.

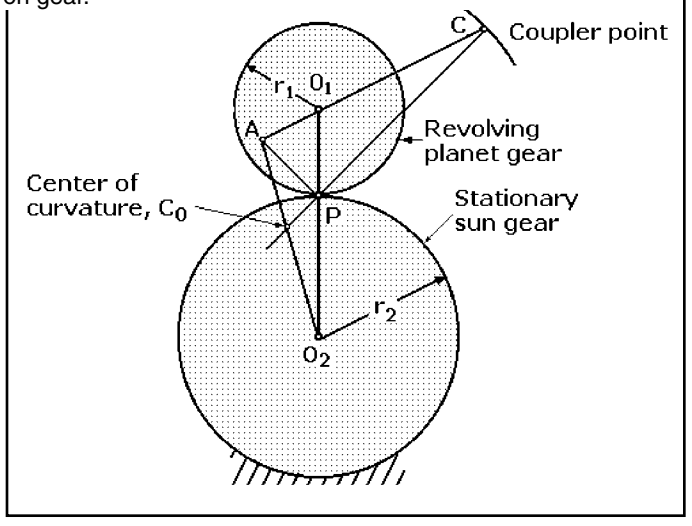

By locating the centers of curvature at various points, one can determine the length of the rocking or reciprocating arm to provide long dwells.

1. Draw a line through points *C* and *P*.
2. Draw a line through points *C* and O_1.
3. Draw a perpendicular to *CP* at *P*. This locates point *A*.
4. Draw line AO_2, to locate C_0, the center of curvature.

Fig. 7 The center of curvature: a gear rolling on a rack

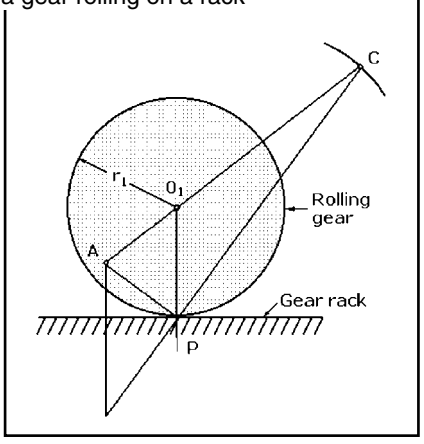

Construction is similar to that of the previous case.

1. Draw an extension of line *CP*.
2. Draw a perpendicular at *P* to locate *A*.
3. Draw a perpendicular from *A* to the straight surface to locate *C*.

Fig. 8 The center of curvature: a gear rolling iside a gear.

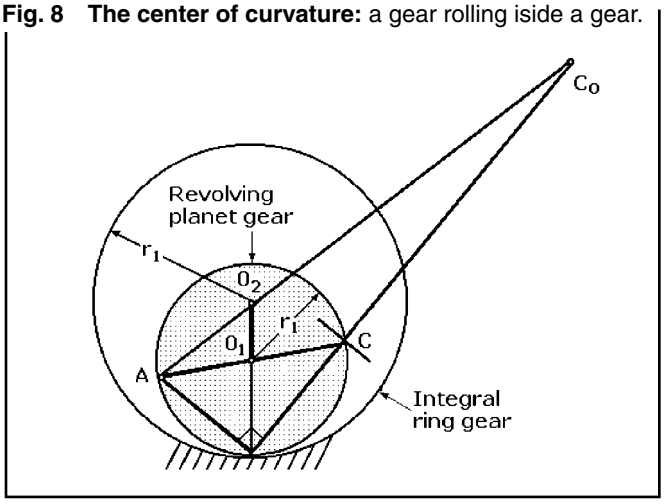

1. Draw extensions of *CP* and CO_1.
2. Draw a perpendicular of *PC* at *P* to locate *A*.
3. Draw AO_2 to locate C_0.

Fig. 9 Analytical solutions.

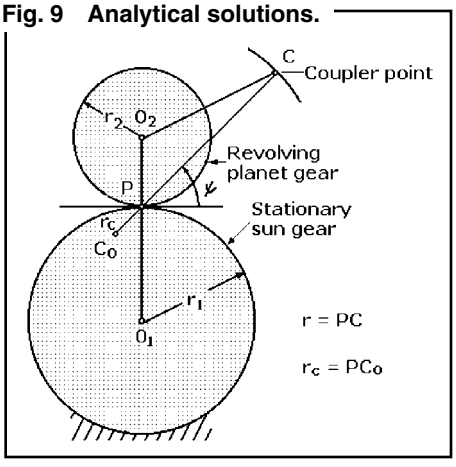

The center of curvature of a gear rolling on an external gear can be computed directly from the Euler-Savary equation:

$$\left(\frac{1}{r}-\frac{1}{r_c}\right)\sin\psi = \text{constant} \qquad (7)$$

where angle ψ and r locate the position of *C*.

By applying this equation twice, specifically to point O_1 and O_2, which have their own centers of rotation, the following equation is obtained:

$$\left(\frac{1}{r_2}-\frac{1}{r_1}\right)\sin 90° = \left(\frac{1}{r}+\frac{1}{r_c}\right)\sin\psi$$

or

$$\frac{1}{r_2}+\frac{1}{r_1} = \left(\frac{1}{r}+\frac{1}{r_c}\right)\sin\psi$$

This is the final design equation. All factors except r_c are known; hence, solving for r_c leads to the location of C_0.

For a gear rolling inside an internal gear, the Euler-Savary equation is:

$$\left(\frac{1}{r}+\frac{1}{r_c}\right)\sin\psi = \text{constant}$$

which leads to:

$$\frac{1}{r_2}-\frac{1}{r_1} = \left(\frac{1}{r}-\frac{1}{r_c}\right)\sin\psi$$

DESIGNING CRANK-AND-ROCKER LINKS WITH OPTIMUM FORCE TRANSMISSION

Four-bar linkages can be designed with a minimum of trial and error by a combination of tabular and iteration techniques.

The determination of optimum crank-and-rocker linkages has most effectively been performed on a computer because of the complexity of the equations and calculations involved. Thanks to the work done at Columbia University's Department of Mechanical and Nuclear Engineering, all you need now is a calculator and the computer-generated tables presented here. The computations were done by Mr. Meng-Sang Chew, at the university.

A crank-and-rocker linkage, *ABCD*, is shown in the first figure. The two extreme positions of the rocker are shown schematically in the second figure. Here ψ denotes the rocker swing angle and ϕ denotes the corresponding crank rotation, both measured counterclockwise from the extended dead-center position, AB_1C_1D.

The problem is to find the proportions of the crank-and-rocker linkage for a given rocker swing angle, ψ, a prescribed corresponding crank rotation, ϕ, and optimum force transmission. The latter is usually defined in terms of the transmission angle, m, the angle μ between coupler *BC* extended and rocker *CD*.

Considering static forces only, the closer the transmission angle is to 90º, the greater is the ratio of the driving component of the force exerted on the rocker to the component exerting bearing pressure on the rocker. The control of transmission-angle variation becomes especially important at high speeds and in heavy-duty applications.

How to find the optimum. The steps in the determination of crank-and-rocker proportions for a given rocker swing angle, corresponding crank rotation, and optimum transmission, are:

- Select (ψ, ϕ) within the following range:
  $0º < \psi < 180º$
  $(90º + 1/2\ \psi) < \phi < (270º + 1/2\ \psi)$
- Calculate: $t = \tan 1/2\ \phi$
  $u = \tan 1/2(\phi - \psi)$
  $v = \tan 1/2\ \psi$

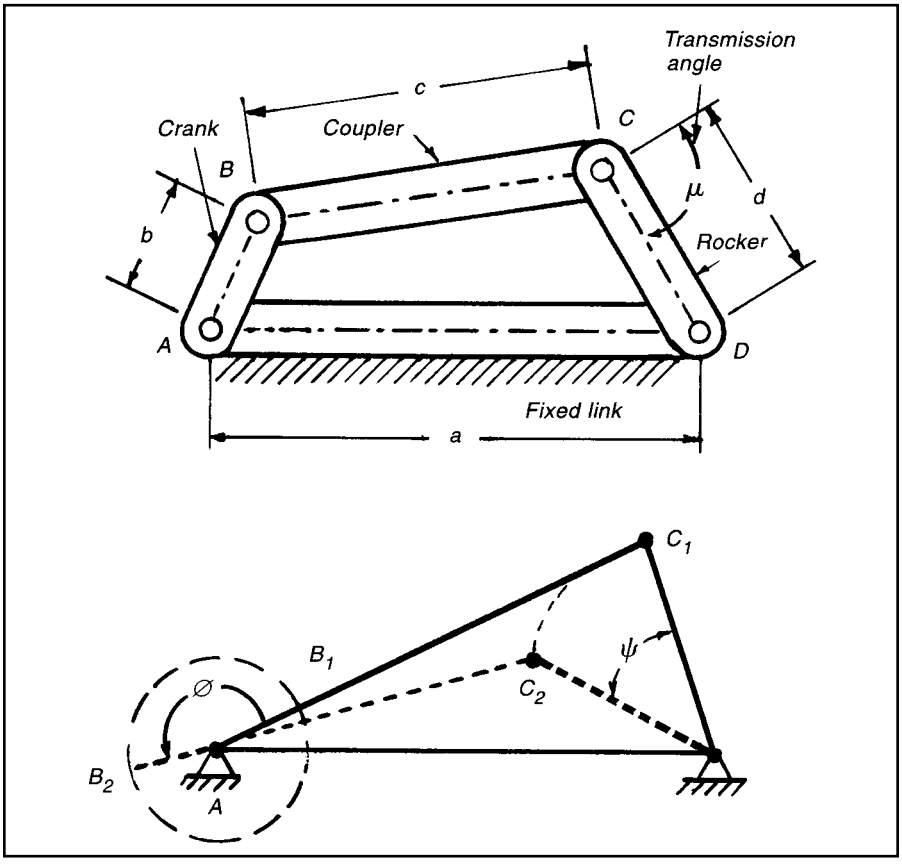

The optimum solution for the classic four-bar crank-and-rocker mechanism problem can now be obtained with only the accompanying table and a calculator.

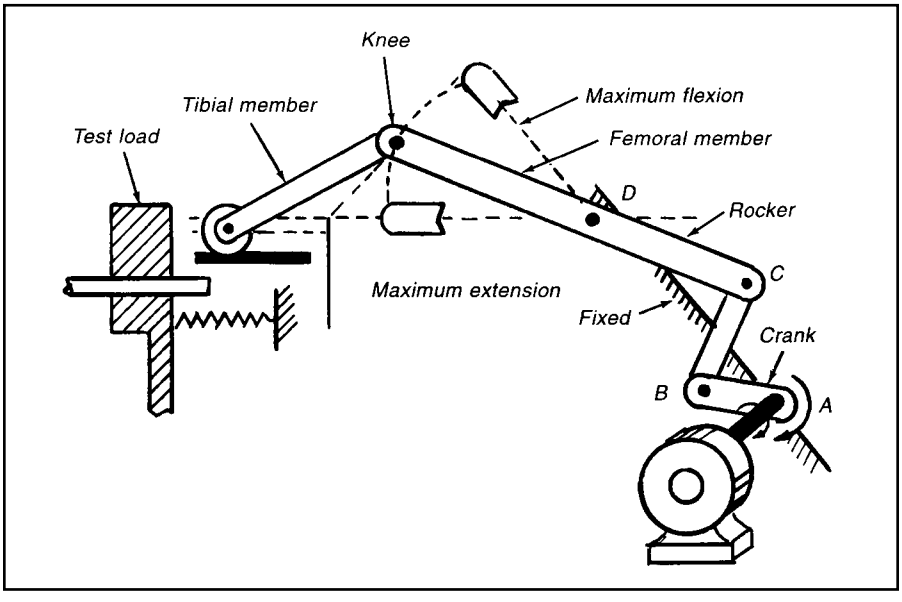

An example in this knee-joint tester designed and built by following the design and calculating procedures outlined in this article.

- Using the table, find the ratio λ_{opt} of coupler to crank length that minimizes the transmission-angle deviation from 90º. The most practical combinations of (ψ, ϕ) are included in the table. If the (ψ, ϕ) combination is not included, or if $\phi = 180º$, go to next steps (a,b,c):
- (a) If $\phi \neq 180º$ and (ψ, ϕ) fall outside the range given in the table, determine the arbitrary intermediate value Q from the equation:
  $Q^3 + 2Q^2 - t^2Q - (t^2/u^2)(1 + t^2) = 0$
  where $(1/u^2 < Q < t^2)$.

This is conveniently accomplished by numerical iteration:

Set $$Q_1 = \tfrac{1}{2}\left(t^2 + \frac{1}{u^2}\right)$$

Calculate Q_2, Q_3, . . . from the recursion equation:

$$Q_{i+1} = \frac{2Q_i^2(Q_i + 1) + (t^2/u^2)(1 + t^2)}{Q_i(3Q_i + 4) - t^2}$$

Iterate until the ratio $[(Q_{i+1} - Q_i)/Q_i]$ is sufficiently small, so that you obtain the desired number of significant figures. Then:

$$\lambda_{opt} = t^2/Q$$

(b) If $\phi \neq 180º$ and the determination of λ_{opt} requires interpolation between two entries in the table, let $Q_1 = t^2\lambda^2$, where λ corresponds to the nearest entry in the table, and continue as in (a) above to determine Q and λ_{opt}. Usually one or two iterations will suffice.

(c) $\phi = 180º$. In this case, $a^2 + b^2 = c^2 + d^2$; $\psi = 2 \sin^{-1}(b/d)$; and the maximum deviation, Δ, of the transmission angle from 90º is equal to $\sin^{-1}(ab/cd)$.

- Determine linkage proportions as follows:

$$(a')^2 = \frac{u^2 + \lambda_{opt}^2}{1 + u^2}$$

$$(b')^2 = \frac{v^2}{1 + v^2}$$

$$(c')^2 = \frac{\lambda_{opt}^2 v^2}{1 + v^2}$$

$$(d')^2 = \frac{t^2 + \lambda_{opt}^2}{1 + t^2}$$

Then: $a = ka'$; $b = kb'$; $c = kc'$; $d = kd'$

where k is a scale factor, such that the length of any one link, usually the crank, is equal to a design value. The max devi-

Optimum values of lambda ratio for given ø and ψ

ø deg	ψ, deg 160	162	164	166	168	170	172	174	176	178
10	2.3532	2.4743	2.6166	2.7873	2.9978	3.2669	3.6284	4.1517	5.0119	6.8642
12	2.3298	2.4491	2.5891	2.7570	2.9636	3.2272	3.5804	4.0899	4.9224	6.6967
14	2.3064	2.4239	2.5617	2.7266	2.9293	3.1874	3.5324	4.0283	4.8342	6.5367
16	2.2831	2.3988	2.5344	2.6964	2.8953	3.1479	3.4848	3.9675	4.7482	6.3853
18	2.2600	2.3740	2.5073	2.6664	2.8615	3.1089	3.4380	3.9080	4.6650	6.2427
20	2.2372	2.3494	2.4805	2.6368	2.8282	3.0704	3.3920	3.8499	4.5848	6.1087
22	2.2145	2.3250	2.4540	2.6076	2.7954	3.0327	3.3470	3.7935	4.5077	5.9826
24	2.1922	2.3010	2.4279	2.5789	2.7631	2.9956	3.3030	3.7388	4.4338	5.8641
26	2.1701	2.2773	2.4022	2.5505	2.7314	2.9594	3.2602	3.6857	4.3628	5.7524
28	2.1483	2.2539	2.3768	2.5227	2.7004	2.9239	3.2185	3.6344	4.2948	5.6469
30	2.1268	2.2309	2.3519	2.4954	2.6699	2.8893	3.1779	3.5847	4.2295	5.5472
32	2.1056	2.2082	2.3273	2.4685	2.6401	2.8554	3.1384	3.5367	4.1668	5.4526
34	2.0846	2.1858	2.3032	2.4421	2.6108	2.8223	3.0999	3.4901	4.1066	5.3628
36	2.0640	2.1637	2.2794	2.4162	2.5821	2.7899	3.0624	3.4449	4.0486	5.2773
38	2.0436	2.1420	2.2560	2.3908	2.5540	2.7583	3.0259	3.4012	3.9927	5.1957
40	2.0234	2.1205	2.2330	2.3657	2.5264	2.7274	2.9903	3.3587	3.9388	5.1177
42	2.0035	2.0994	2.2103	2.3411	2.4994	2.6971	2.9556	3.3175	3.8868	5.0430
44	1.9839	2.0785	2.1879	2.3169	2.4728	2.6675	2.9217	3.2773	3.8364	4.9712
46	1.9644	2.0579	2.1659	2.2931	2.4468	2.6384	2.8886	3.2383	3.7877	4.9023
48	1.9452	2.0375	2.1441	2.2696	2.4211	2.6100	2.8563	3.2003	3.7404	4.8358
50	1.9262	2.0174	2.1227	2.2465	2.3959	2.5820	2.8246	3.1632	3.6945	4.7717

ation, Δ, of the transmission angle from 90° is:

$$\sin\Delta = \frac{|(a \pm b)^2 - c^2 - d^2|}{2cd}$$

$0° \le \Delta \le 90°$
+ sign if $\phi < 180°$
− sign if $\phi > 180°$

An actual example. A simulator for testing artificial knee joints, built by the Department of Orthopedic Surgery, Columbia University, under the direction of Dr. N. Eftekhar, is shown schematically. The drive includes an adjustable crank-and-rocker, ABCD. The rocker swing angle ranges from a maximum of about 48° to a minimum of about one-third of this value. The crank is 4 in. long and rotates at 150 rpm. The swing angle adjustment is obtained by changing the length of the crank.

Find the proportions of the linkage, assuming optimum-transmission proportions for the maximum rocker swing angle, as this represents the most severe condition. For smaller swing angles, the maximum transmission-angle deviation from 90° will be less.

Crank rotation corresponding to 48° rocker swing is selected at approximately 170°. Using the table, find $\lambda_{opt} = 2.6100$. This gives $a' = 1.5382$, $b' = 0.40674$, $c' = 1.0616$, and $d' = 1.0218$.

For a 4 in. crank, $k = 4/0.40674 = 9.8343$ and $a = 15.127$ in., $b = 4$ in., $c = 10.440$ in., and $d = 10.049$ in., which is very close to the proportions used. The maximum deviation of the transmission angle from 90° is 47.98°.

This procedure applies not only for the transmission optimization of crank-and-rocker linkages, but also for other crank-and-rocker design. For example, if only the rocker swing angle and the corresponding crank rotation are prescribed, the ratio of coupler to crank length is arbitrary, and the equations can be used with any value of λ_2 within the range $(1, u^2t^2)$. The ratio λ can then be tailored to suit a variety of design requirements, such as size, bearing reactions, transmission-angle control, or combinations of these requirements.

The method also was used to design dead-center linkages for aircraft landing-gear retraction systems, and it can be applied to any four-bar linkage designs that meet the requirements discussed here.

Optimum values of lambda ratio for given ø and ψ

ø deg	ψ, deg 182	184	186	188	190	192	194	196	198	200
10	7.2086	5.3403	4.4560	3.9112	3.5318	3.2478	3.0245	2.8428	2.6911	2.5616
12	7.0369	5.2692	4.4227	3.8969	3.5282	3.2507	3.0317	2.8528	2.7030	2.5748
14	6.8646	5.1881	4.3795	3.8739	3.5174	3.2478	3.0341	2.8589	2.7117	2.5855
16	6.6971	5.1013	4.3287	3.8435	3.5000	3.2392	3.0317	2.8610	2.7171	2.5934
18	6.5371	5.0121	4.2726	3.8071	3.4768	3.2252	3.0245	2.8589	2.7189	2.5982
20	6.3857	4.9226	4.2131	3.7663	3.4487	3.2065	3.0129	2.8528	2.7171	2.5998
22	6.2431	4.8344	4.1518	3.7221	3.4167	3.1837	2.9972	2.8428	2.7117	2.5982
24	6.1090	4.7484	4.0900	3.6759	3.3818	3.1575	2.9780	2.8293	2.7030	2.5934
26	5.9830	4.6652	4.0284	3.6284	3.3447	3.1286	2.9558	2.8127	2.6911	2.5855
28	5.8644	4.5849	3.9676	3.5804	3.3062	3.0976	2.9311	2.7833	2.6763	2.5748
30	5.7527	4.5079	3.9080	3.5324	3.2669	3.0652	2.9045	2.7718	2.6592	2.5616
32	5.6472	4.4339	3.8500	3.4849	3.2272	3.0318	2.8764	2.7484	2.6399	2.5461
34	5.5475	4.3630	3.7936	3.4380	3.1875	2.9979	2.8473	2.7236	2.6190	2.5287
36	5.4529	4.2949	3.7388	3.3920	3.1480	2.9636	2.8175	2.6977	2.5967	2.5097
38	5.3631	4.2296	3.6858	3.3470	3.1089	2.9294	2.7873	2.6711	2.5734	2.4894
40	5.2776	4.1669	3.6345	3.3031	3.0705	2.8953	2.7570	2.6440	2.5492	2.4680
42	5.1960	4.1067	3.5848	3.2602	3.0327	2.8615	2.7266	2.6166	2.5246	2.4459
44	5.1180	4.0487	3.5367	3.2185	2.9956	2.8282	2.6964	2.5891	2.4996	2.4232
46	5.0432	3.9928	3.4901	3.1779	2.9594	2.7954	2.6665	2.5617	2.4744	2.4001
48	4.9715	3.9389	3.4450	3.1384	2.9239	2.7631	2.6369	2.5344	2.4491	2.3767
50	4.9025	3.8869	3.4012	3.0999	2.8893	2.7314	2.6076	2.5073	2.4239	2.3533

DESIGN CURVES AND EQUATIONS FOR GEAR-SLIDER MECHANISMS

What is a gear-slider mechanism? It is little more than a crank-and-slider with two gears meshed in line with the crank (Fig. 1). But, because one of the gears (planet gear, 3) is prevented from rotating because it is attached to the connecting rod, the output is taken from the sun gear, not the slider. This produces a variety of cyclic output motions, depending on the proportions of the members.

In his investigation of the capabilities of the mechanism, Professor Preben Jensen of Bridgeport, Connecticut derived the equations defining its motion and acceleration characteristics. He then devised some variations of his own (Figs. 5 through 8). These, he believes, will outperform the parent type. Jensen illustrated how the output of one of the new mechanisms, Fig. 8, can come to dead stop during each cycle, or progressively oscillate to new positions around the clock. A machine designer, therefore, can obtain a wide variety of intermittent motions from the arrangement and, by combining two of these units, he can tailor the dwell period of the mechanism to fit the automatic feed requirements of a machine.

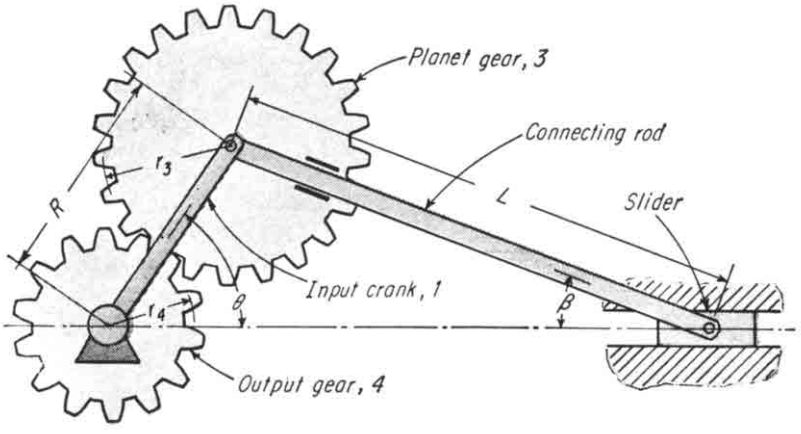

Fig. 1 A basic gear-slider mechanism. It differs from the better known three-gear drive because a slider restricts the motion of the planet gear. The output is taken from the gear, which is concentric with the input shaft, and not from the slider.

Symbols

L = Length of connecting rod, in.

r_3 = radius of gear fixed to connecting rod, in.

r_4 = radius of output gear, in.

R = length of crank, in.

α = angular acceleration of the input crank, rad/sec^2

β = connecting rod displacement, deg

γ = output rotation, deg

θ = input rotation, deg

θ_o = crank angle rotation during which the output gear reverses its motion, deg

ϕ = angle through which the output gear rotates back

ω = angular velocity of input crank, rad/sec

A single prime mark denotes angular velocity, rad/sec; double prime marks denote angular acceleration, rad/sec^2.

The Basic Form

The input motion is to crank 1, and the output motion is from gear 4. As the crank rotates, say counterclockwise, it causes planet gear 3 to oscillate while following a satellite path around gear 4. This imparts a varying output motion to gear 4, which rotates twice in the counterclockwise direction (when $r_3 = r_4$) for every revolution of the input.

Jensen's equations for angular displacement, velocity, and acceleration of gear 4, when driven at a speed of ω by crank 1, are as follows:

Angular Displacement

$$\gamma = \theta + \frac{r_3}{r_4}(\theta + \beta) \tag{1}$$

where β is computed from the following relationship (see the list of symbols in this article):

$$\sin\beta = \frac{R}{L}\sin\theta \tag{2}$$

Angular Velocity

$$\gamma' = \omega + \frac{r_3}{r_4}(\omega + \beta') \tag{3}$$

where

$$\frac{\beta'}{\omega} = \frac{R}{L}\frac{\cos\theta}{\left[1-\left(\frac{R}{L}\right)^2\sin^2\theta\right]^{1/2}} \tag{4}$$

Angular Acceleration

$$\gamma'' = \alpha + \frac{r_3}{r_4}(\alpha + \beta'') \tag{5}$$

where

$$\frac{\beta''}{\omega^2} = \frac{R}{L}\frac{\sin\theta\left[\left(\frac{R}{L}\right)^2 - 1\right]}{\left[1-\left(\frac{R}{L}\right)^2\sin^2\theta\right]^{3/2}} \tag{6}$$

For a constant angular velocity, Eq. 5 becomes

$$\gamma'' = \frac{r_3}{r_4}\beta'' \tag{7}$$

Design Charts

The equations were solved by Professor Jensen for various *L/R* ratios and positions of the crank angle θ to obtain the design charts in Figs. 2, 3, and 4. Thus, for a mechanism with

L = 12 in. $r_3 = 2.5$
R = 4 in. $r_4 = 1.5$
ω = 1000 per second
= radians per second

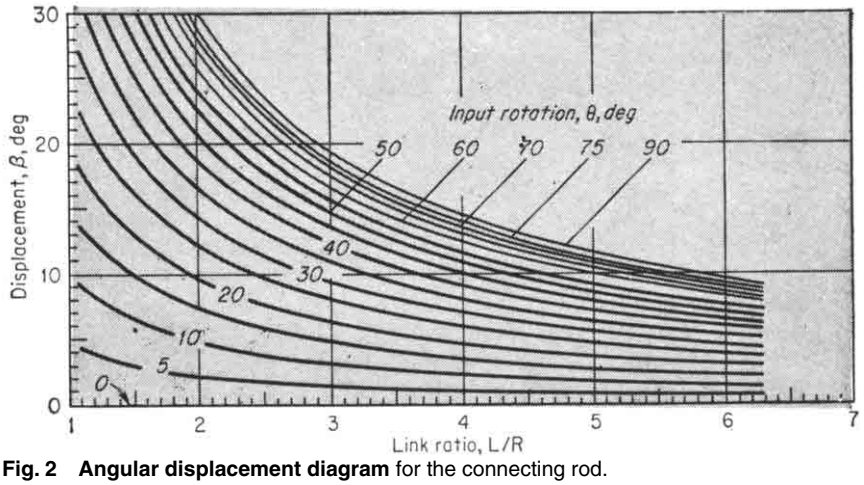

Fig. 2 Angular displacement diagram for the connecting rod.

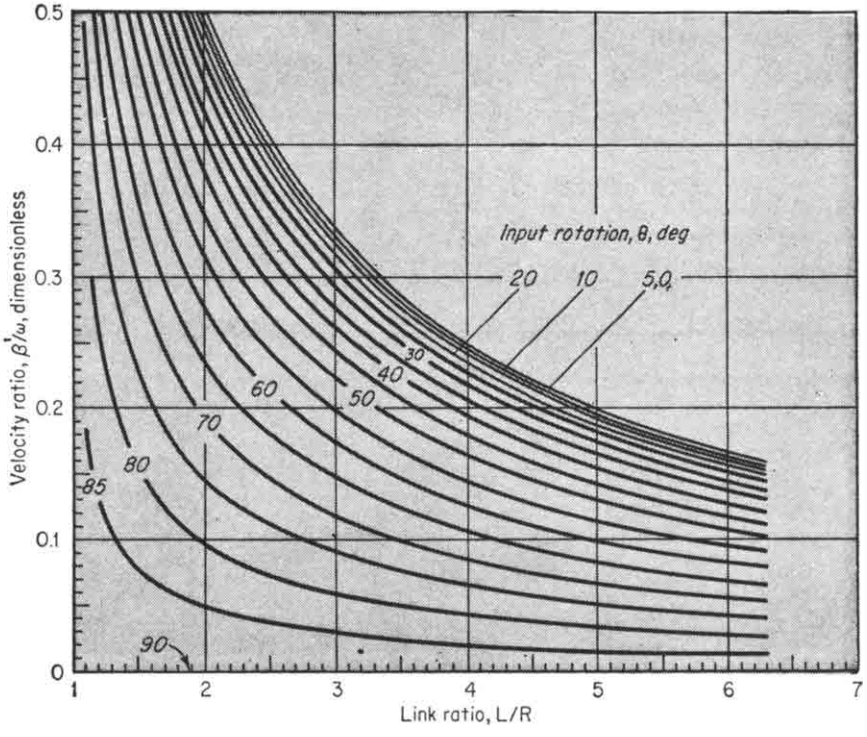

Fig. 3 Angular velocity curves for various crank angles.

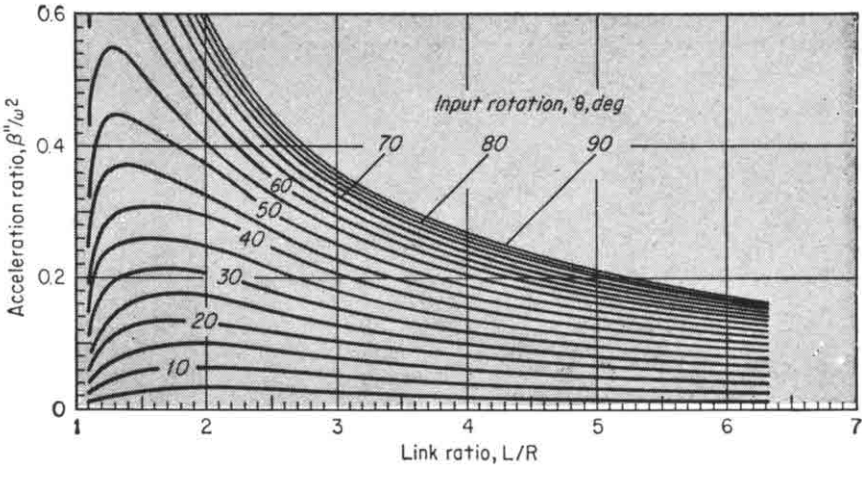

Fig. 4 Angular acceleration curves for various crank angles.

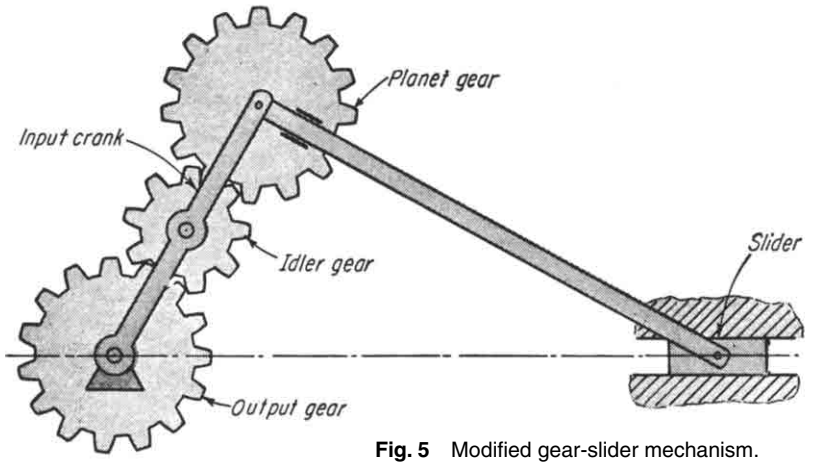

Fig. 5 Modified gear-slider mechanism.

the output velocity at crank angle $\theta = 60°$ can be computed as follows:

$$L/R = 12/4 = 3$$

From Fig. 3 $\beta'/\omega = 0.175$

$$\beta' = 0.175(1000)$$
$$= 175 \text{ radians per second}$$

From Eq. 3

$$\gamma = 2960 \text{ radians per second}$$

Three-Gear Variation

One interesting variation, shown in Fig. 5, is obtained by adding idler gear 5 to the drive. If gears 3 and 4 are then made equal in side, output gear 4 will then oscillate with exactly the same motion as connecting rod 2.

One use for this linkage, Jensen said, is in machinery where a sleeve is to ride concentrically over an input shaft, and yet must oscillate to provide a reciprocating motion. The shaft can drive the sleeve with this mechanism by making the sleeve part of the output gear.

Internal-Gear Variations

By replacing one of the external gears of Fig. 1 with an internal one, two mechanisms are obtained (Figs. 6 and 7) which have wider variable output abilities. But it is the mechanism in Fig. 7 that interested Jensen. This could be proportioned to give either a dwell or a progressive oscillation, that is, one in which the output rotates forward, say 360º, turns back to 30º, moves forward 30º, and then proceeds to repeat the cycle by moving forward again for 360º.

In this mechanism, the crank drives the large ring gear 3 which is fixed to the connecting rod 2. Output is from gear 4. Jensen derived the following equations:

Output Motion

$$\omega_4 = -\left(\frac{L - R - r_4}{Lr_4}\right) R\omega_1 \qquad (8)$$

When $r_4 = L - R$, then $\omega_4 = 0$ from Eq. 8, and the mechanism is proportioned to give instantaneous dwell. To obtain a progressive oscillation, r_4 must

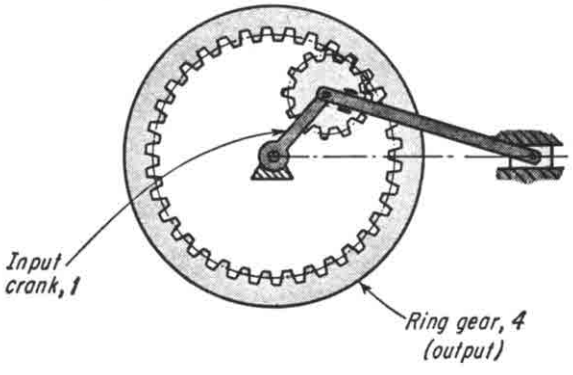

Fig. 6 A ring-gear and slider mechanism. The ring gear is the output and it replaces the center gear in Fig. 1.

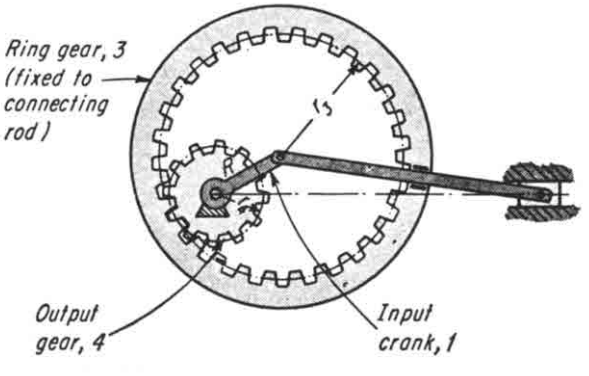

Fig. 7 A more practical ring-gear and slider arrangement. The output is now from the smaller gear.

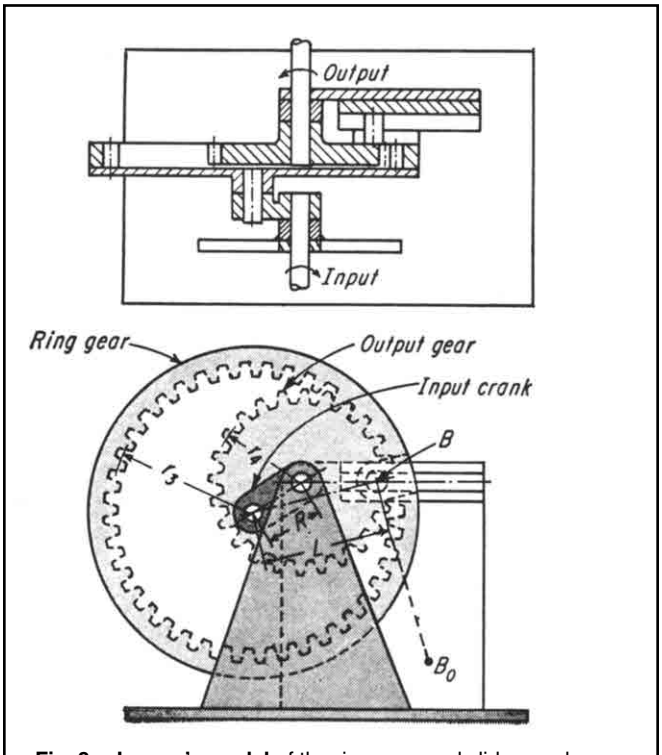

Fig. 8 Jensen's model of the ring-gear and slider mechanism shown in Fig. 7. A progressive oscillation motion is obtained by making r_4 greater than *L-R*.

be greater than $L - R$, as shown in Jensen's model (Fig. 8).

If gear 4 turns back and then starts moving forward again, there must be two positions where the motion of gear 4 is zero. Those two mechanisms are symmetrical with respect to A_0B. If θ_0 equals the crank-angle rotation (of input), during which the output gear reverses its motion, and ϕ equals the angle through which gear 4 rotates back, then

$$\cos\frac{\theta_0}{2} = \left[\frac{L^2 - R^2}{r_4(2R + r_4)}\right]^{1/2} \qquad (9)$$

and

$$\gamma = \theta_0 - \frac{r_3}{r_4}(\theta_0 - \beta_0) \qquad (10)$$

where

$$\sin\beta_0 = \frac{R}{L}\sin\frac{\theta_0}{2} \qquad (11)$$

Chart for Proportioning

The chart in Fig. 9 helps proportion the mechanism of Fig. 8 to provide a specific kind of progressive oscillation. It is set up for R equals 1 in. For other values of R, convert the chart values for r_4 proportionally, as shown below.

For example, assume that the output gear, during each cycle, is to rotate back 9.2°. Thus ϕ = 9.2°. Also given is R = 0.75 in. and L = 1.5 in. Thus L/R = 2.

From the right side of the chart, go to the ϕ-curve for L = 2, then upward to the θ_0-curve for L = 2 in. Read θ_0 = 82° at the left ordinate.

Now return to the second intersection point and proceed upward to read on the abscissa scale for L = 2, a value of r_4 = 1.5. Since R = 0.75 in., and the chart is for R 1, convert r_4 as follows: r_4 = 0.75 (1.5) = 1.13 in.

Thus, if the mechanism is built with an output gear of radius r_4 = 1.13 in., then during 82° rotation of the crank, the output gear 4 will go back 9.2°. Of course, during the next 83°, gear 4 will have reversed back to its initial position—and then will keep going forward for the remaining 194° of the crank rotation.

Future Modifications

The mechanism in Fig. 8 is designed to permit changing the output motion easily from progressive oscillation to instantaneous dwell or nonuniform CW or CCW rotation. This is accomplished by shifting the position of the pin which acts as the sliding piece of the centric slider crank. It is also possible to use an eccentric slider crank, a four-bar linkage, or a sliding-block linkage as the basic mechanism.

Two mechanisms in series will give an output with either a prolonged dwell or two separate dwells. The angle between the separated dwells can be adjusted during its operation by interposing a gear differential so that the position of the output shaft of the first mechanism can be changed relative to the position of the input shaft of the second mechanism.

The mechanism can also be improved by introducing an additional link, B-B_0, to guide pin B along a circular arc instead of a linear track. This would result in a slight improvement in the performance of the mechanism.

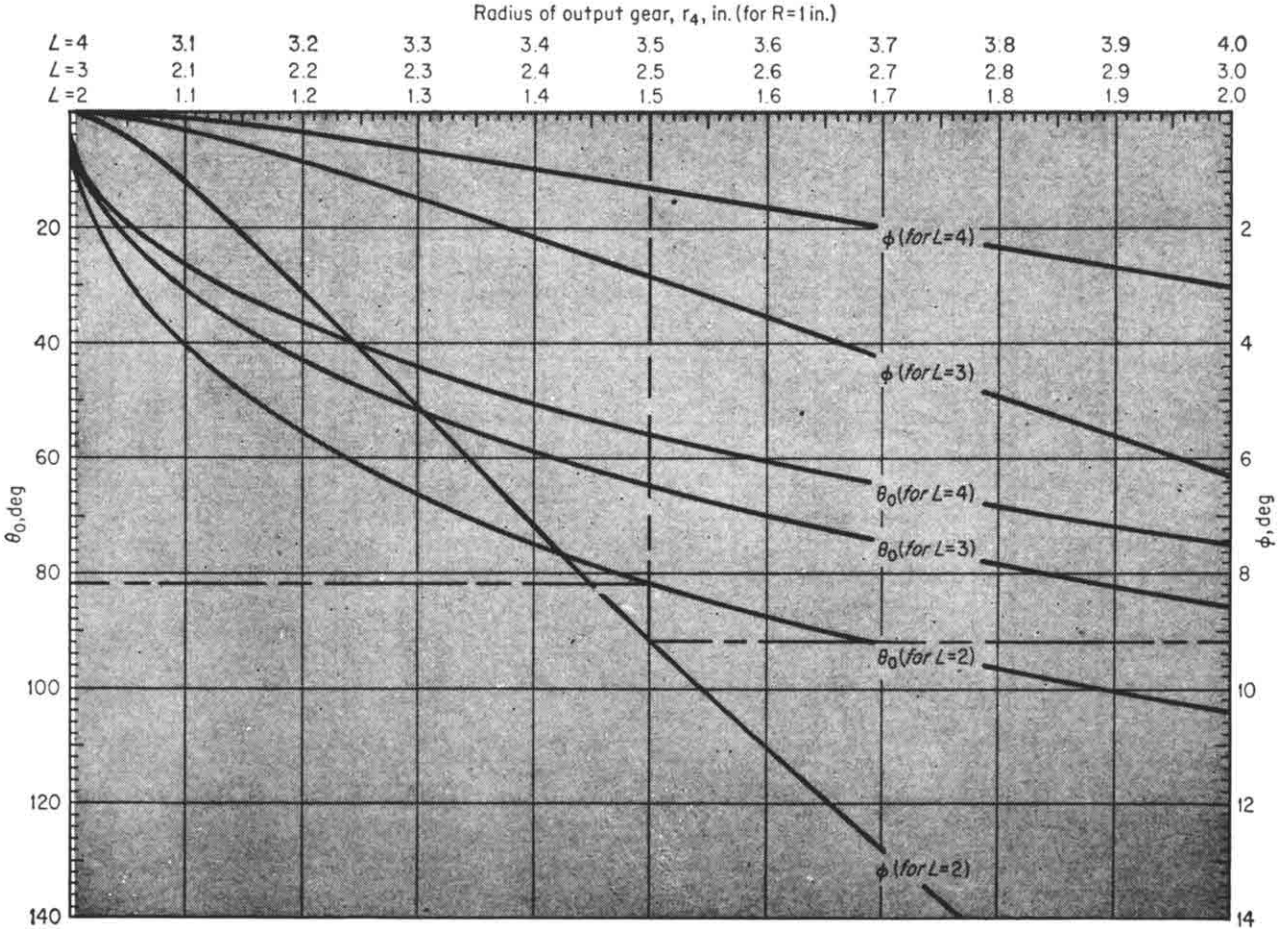

Fig. 9 **A chart** for proportioning a ring-gear and slider mechanism.

DESIGNING SNAP-ACTION TOGGLES

Theory, formulas, and design charts are presented for determining toggle dimensions to maximize snap-action.

Over-centering toggle mechanisms, as shown in Fig. 1, are widely used in mechanical and electrical switches, latch mechanisms and mechanical overload controls. These toggles also serve as: (1) detents (for holding other parts in selected position); (2) overload devices in mechanical linkages (they shift to the opposite position when sufficiently loaded); and (3) energy-storage devices.

Two applications, shown in Fig. 2, illustrate the snap-action of a toggle. As the toggle passes dead center, it is snapped ahead of the actuating force by the toggle spring. In most applications, the objective is to obtain maximum snap-action.

Snap-action is a function of the elongation per length of the toggle spring as it moves over dead center. Elongation at dead center is equal to:

$$J = K - H \tag{1}$$

The elongation e in percent of length is equal to:

$$e = (100)J/S \tag{2}$$

Because the resisting force of the spring increases with elongation but decreases with an increase in length, the ratio J/S should be as large as possible within the capacity of the spring for the best snap-action performance.

The ratio J/S as a function of angle θ can be derived as follows:

$$H = S - S\cos\varphi \tag{3}$$

and

$$K = A - A\cos\theta \tag{4}$$

Substituting Eqs. (3) and (4) into Eq. (1),

$$J = A(1 - \cos\theta) - S(1 - \cos\varphi) \tag{5}$$

or

$$J/S = (A/S)(1 - \cos\theta) - (1 - \cos\varphi) \tag{6}$$

The relationship between θ and ϕ is:

$$L = A\sin\theta = S\sin\varphi$$

or

$$\sin\varphi = (A/S)(\sin\theta) \tag{7}$$

By trigonometric identity,

$$\sin\theta = (1 - \cos^2\theta)^{1/2} \tag{8}$$

Substituting Eq. (8) into Eq. (7) and squaring both sides,

$$\sin\varphi = (A/S)^2(1 - \cos^2\theta) \tag{9}$$

By trigonometric identity,

$$\cos\varphi = (1 - \sin^2\varphi)^{1/2} \tag{10}$$

Substituting Eq. (9) into Eq. (10),

$$\cos\varphi = [1 - (A/S)^2 + (A/S)^2\cos^2\theta]^{1/2} \tag{11}$$

and Eq. (11) into Eq. (6),

$$J/S = (A/S)(1 - \cos\theta) - 1 + [1 - (A/S)(1 - \cos\theta) - 1 - (A/S)^2\cos^{1/2} \tag{12}$$

Eq. (12) can be considered to have only three variables: (1) the spring elongation ratio J/S; (2) the toggle arm to spring length ratio, A/S; and (3) the toggle arm angle θ.

A series of curves are plotted from Eq. (12) showing the relationship between J/S and A/S for various angles of θ. The curves are illustrated in Fig. 3; for greater accuracy each chart has a different vertical scale.

Maximum Snap-Action

Maximum snap-action for a particular angle occurs when J/S is a maximum. This can be determined by setting the first derivative of Eq. (12) equal to zero and solving for A/S.

Differentiating Eq. (12),

$$\frac{d(J/S)}{d(A/S)} = 1 - \cos\theta + \frac{[-2(A/S) + 2(A/S)(\cos^2\theta)]}{2[1 - (A/S)^2 + (A/S)^2\cos^2\theta]^{1/2}} \tag{13}$$

Setting Eq. (13) Equal to zero and rearranging terms,

$$\frac{\cos\theta - 1}{\cos^2\theta - 1} = \frac{A/S}{(A/S)[(S/A)^2 - 1 + \cos^2\theta]^{1/2}} \tag{14}$$

Cross-multiplying, squaring, and simplifying,

$$(S/A)^2 - 1 + \cos^2\theta = \cos^2\theta + 2\cos\theta + 1$$

Reducing,

$$(S/A)^2 = 2\cos\theta + 2$$

and finally simplifying to the following equation is A/S when J/S is a maximum:

$$A/S = [2(\cos\theta + 1)]^{-1/2} \tag{15}$$

The maximum value of J/S can be determined by substituting Eq. (15) into Eq. (12):

$$J/S_{max} = \frac{1 - \cos\theta}{[2(\cos\theta + 1)]^{1/2}} - 1 + \left[1 - \frac{1}{2(\cos\theta + 1)} + \frac{\cos^2\theta}{2(\cos\theta + 1)}\right]^{1/2} \tag{16}$$

which is simplified into the following expression:

$$J/S_{max} = \frac{2 - [2(\cos\theta + 1)]^{1/2}}{[2(\cos\theta + 1)]^{1/2}} \tag{17}$$

The locus of points of J/S_{max} is a straight line function as shown in Fig. 3. It can be seen from Eq. (15) that the value of A/S at J/S_{max} varies from 0.500 when $\theta = 0$ to 0.707 when $\theta = 90°$. This relatively small range gives a quick rule-of-thumb to check if a mechanism has been designed close to the maximum snap-action point.

Elongation of the spring, Eq. (2), is based on the assumption that the spring is installed in its free length S with no initial elongation. For a spring with a free length E smaller than S, the total elongation in percent when extended to the dead center position is:

$$e = 100[(S/E)(1 + J/S) - 1] \tag{18}$$

The relationship between ϕ and θ at the point of maximum snap-action for any value of θ is:

$$\theta = 2\varphi \tag{19}$$

This can be proved by substituting Eqs. (9) and (11) into the trigonometric identity:

$$\cos 2\varphi = \cos^2\varphi - \sin^2\varphi \tag{20}$$

and comparing the resulting equation with one obtained by solving for $\cos\theta$ in Eq. (15). This relationship between the angles is another way to evaluate a toggle mechanism quickly.

Design Procedure

A toggle is usually designed to operate within certain space limitations. When the dimensions X and W, as shown in Fig. 4, are known, the angle θ resulting in maximum snap-action can be determined as follows:

$$A\sin\theta = S\sin\varphi = W/2 \tag{21}$$

Substituting Eq. (19) into Eq. (21),

$$A\sin\theta = S\sin(\theta/2) = W/2 \tag{22}$$

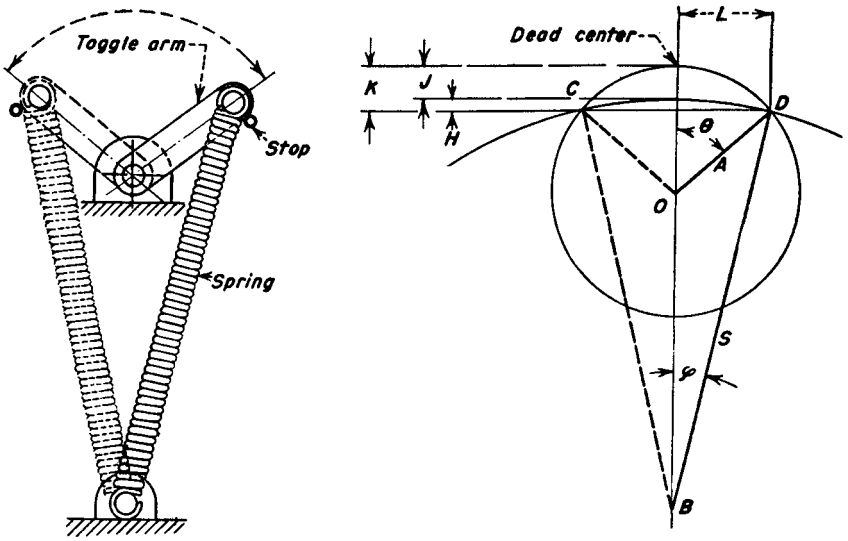

Symbols

A = length of toggle arm
S = free length of toggle spring in detented positions
θ = angle swept by toggle arm moving from detented to dead center position
φ = angle swept by toggle spring in moving from detented to dead center position
CD = chordal distance between detent points
L = chordal distance between detent point and dead center
K = height of arc swept by toggle arm
O = pivot point of toggle arm
B = pivot point of toggle spring

Fig. 1 The design analysis for a snap-action or over-centering toggle employing a link and spring. The mechanical view is shown at left, and the kinematic representation is at right.

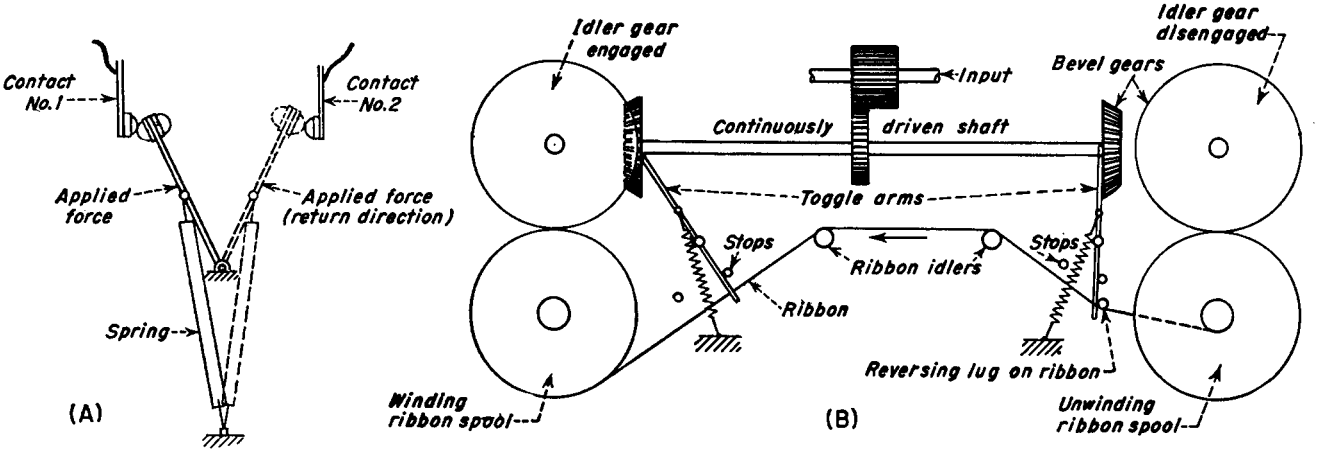

Fig. 2 Typical applications of toggles: (A) snap-action switches; (B) ribbon reversing mechanical for typewriters and calculators. The toggle in (B) is activated by a lug on the ribbon. As it passes dead center it is snapped ahead of the lug by the toggle spring, thus shifting the shaft and reversing the direction of the ribbon before next key is struck.

From Fig. 4:

$$X = S\cos(\theta/2) + A - A\cos\theta \quad (23)$$

Substituting Eq. (22) into Eq. (23),

$$X = \frac{W\cos(\theta/2)}{2\sin(\theta/2)} + \frac{W}{2\sin\theta} - \frac{W\cos\theta}{2\sin\theta} \quad (24)$$

Converting to half-angle functions and simplifying,

$$X = W/[2\sin(\theta/2)\cos(\theta/2)] \quad (25)$$

Using the trigonometric identity,

$$\sin\theta = 2\sin(\theta/2)\cos(\theta/2) \quad (26)$$

Eq. (25) becomes:

$$X = W/\sin\theta$$

or

$$\sin\theta = W/X \quad (27)$$

Solving for θ permits the ratios A/S and J/S to be determined from the charts in Fig. 3, when using the J/S (max) line. The values of S and A can then be obtained from Eq. (22).

It can be seen from Fig. 3 that $\theta = 90°$ results in maximum snap-action. Substitution of the sin of 90° in Eq. (27) results in $W = X$; in other words, the most efficient space configuration for a toggle is a square.

EDITOR'S NOTE—In addition to the toggles discussed here, the term "toggle" is applied to a mechanism containing two links that line up in a straight line at one point in their motion, giving a high mechanical advantage.

Toggles of this kind offer: (1) a high mechanical advantage, (2) a high velocity ratio, and (3) a variable mechanical advantage.

Fig. 3 Design charts for evaluating toggle arm and spring length for maximum spring elongation. Chart (B) is an extension of chart (A).

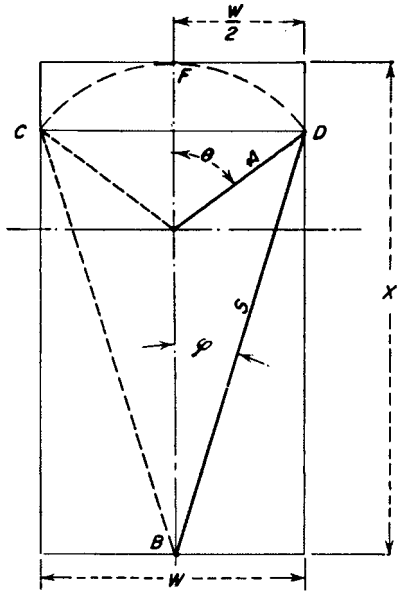

Fig. 4 Designing a toggle to lie within space boundaries *W* and *X*. It can be shown that for maximum snap-action, sin θ = *X*/*W*.

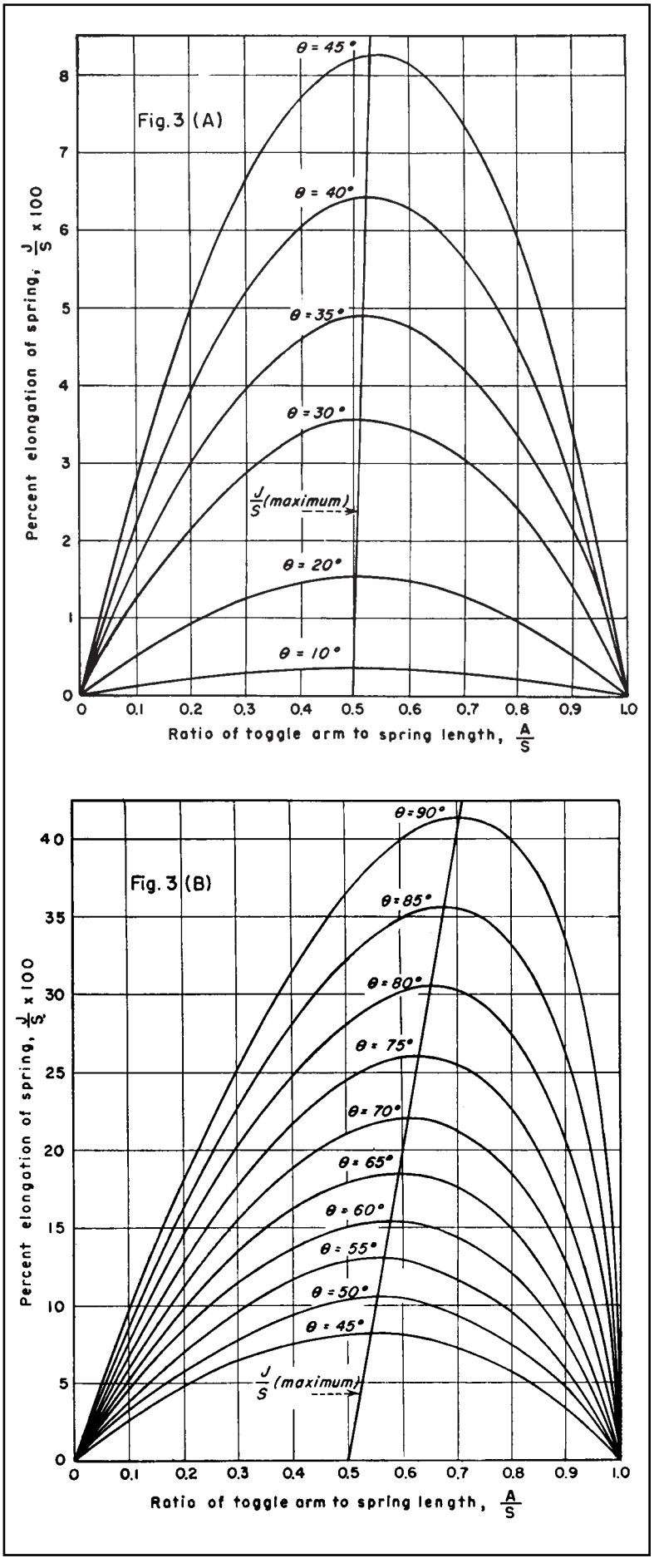

FEEDER MECHANISMS FOR ANGULAR MOTIONS

How to use four-bar linkages to generate continuous or intermittent angular motions required by feeder mechanisms

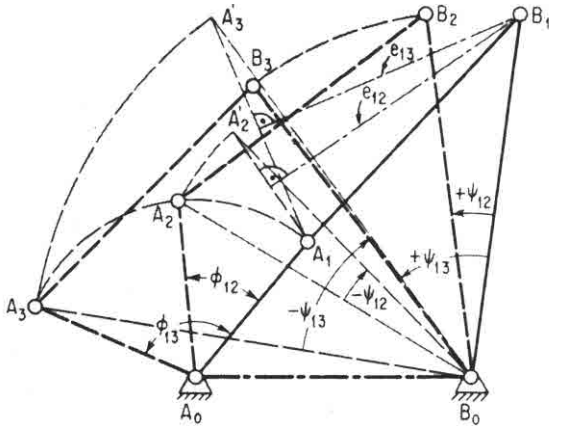

Fig. 1 Four-bar linkage synchronizes two angular movements, ϕ_{12} and ϕ_{13}, with ψ_{12}, and ψ_{14}.

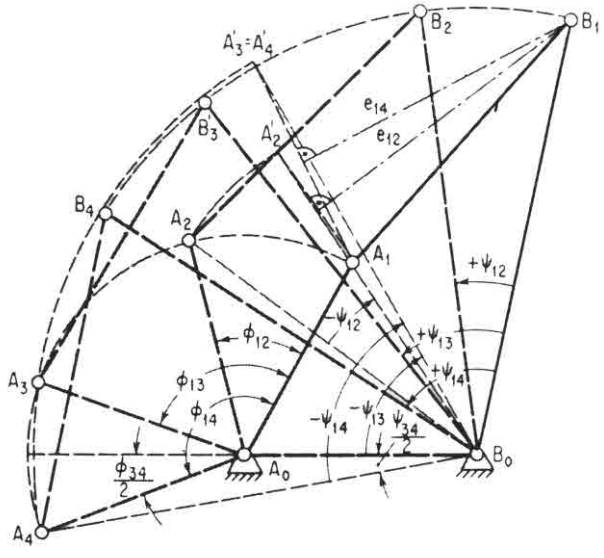

Fig. 2 Three angular positions, ϕ_{12}, ϕ_{13}, ϕ_{14}, are synchronized by four-bar linkage here with ψ_{12}, ψ_{13}, and ψ_{14}.

In putting feeder mechanisms to work, it is often necessary to synchronize two sets of angular motions. A four-bar linkage offers one way. For example, in Fig. 1 two angular motions, ϕ_{12} and ϕ_{13}, must be synchronized with two others, ψ_{12} and ψ_{13}, about the given pivot points A_0 and B_0 and the given crank length A_0A. This means that crank length B_0B. must be long enough so that the resulting four-bar linkage will coordinate angular motions ϕ_{12} and ϕ_{13} with ψ_{12} and ψ_{13}. The procedure is:

1. Obtain point A'_2 by revolving A_2 about B_0 through angle $-\psi_{12}$ but in the opposite direction.
2. Obtain point A'_3 similarly by revolving A_3 about B_0 through angle $-\psi_{13}$.
3. Draw lines $A_1A'_2$ and $A_1A'_3$ and the perpendicular bisectors of the lines which intersect at desired point B_1.
4. The quadrilateral $A_0A_1B_1B_0$ represents the four-bar linkage that will produce the required relationship between the angles ϕ_{12}, ϕ_{13}, and ψ_{12}, ψ_{13}.

Three angles with four relative positions can be synchronized in a similar way. Figure 2 shows how to synchronize angles ψ_{12}, ψ_{13},ψ_{14} with corresponding angles ψ_{12}, ψ_{13}, and ψ_{14}, using freely chosen pivot points A_0 and B_0. In this case, crank length A_0A as well as B_0B is to be determined, and the procedure is:

1. Locate pivot points A_0 and B_0 on a line those bisects angle $A_3A_0A_4$, the length A_0B_0 being arbitrary.
2. Measure off ½ of angle $B_3B_0B_4$ and with this angle draw B_0A_4 which establishes crank length A_0A at intersection of A_0A_4. This also establishes points A_3, A_2 and A_1.
3. WithB_0 as center and B_0B_4 as radius mark off angles $-\psi_{14}$, $-\psi_{13}$, $-\psi_{12}$, the negative sign indicating they are in opposite sense to ψ_{14}, ψ_{13} and ψ_{12}. This establishes points A'_2, A'_3 and A'_4, but here A'_3 and A'_4 coincide because of symmetry of A_3 and A_4 about A_0B_0.
4. Draw lines $A_1A'_2$ and $A_1A'_4$, and the perpendicular bisectors of these lines, which intersect at the desired point B_1.
5. The quadrilateral $A_0A_1B_0B_1$ represents the four-bar linkage that will produce the required relationship between the angles ϕ_{12}, ϕ_{13}, ϕ_{14}, and ψ_{12}, ψ_{13}, ψ_{14}.

The illustrations show how these angles must be coordinated within the given space. In Fig. 3A, input angles of the crank must be coordinated with the output angles of the forked escapement. In Fig. 3B, input angles of the crank are coordinated with the output angles of the tilting hopper. In Fig. 3C, the input angles of the crank are coordinated with the output angles of the segment. In Fig. 3D, a box on a conveyor is tilted 90º by an output crank, which is actuated by an input crank through a coupler. Other mechanisms shown can also coordinate the input and output angles; some have dwell periods between the cycles, others give a linear output with dwell periods.

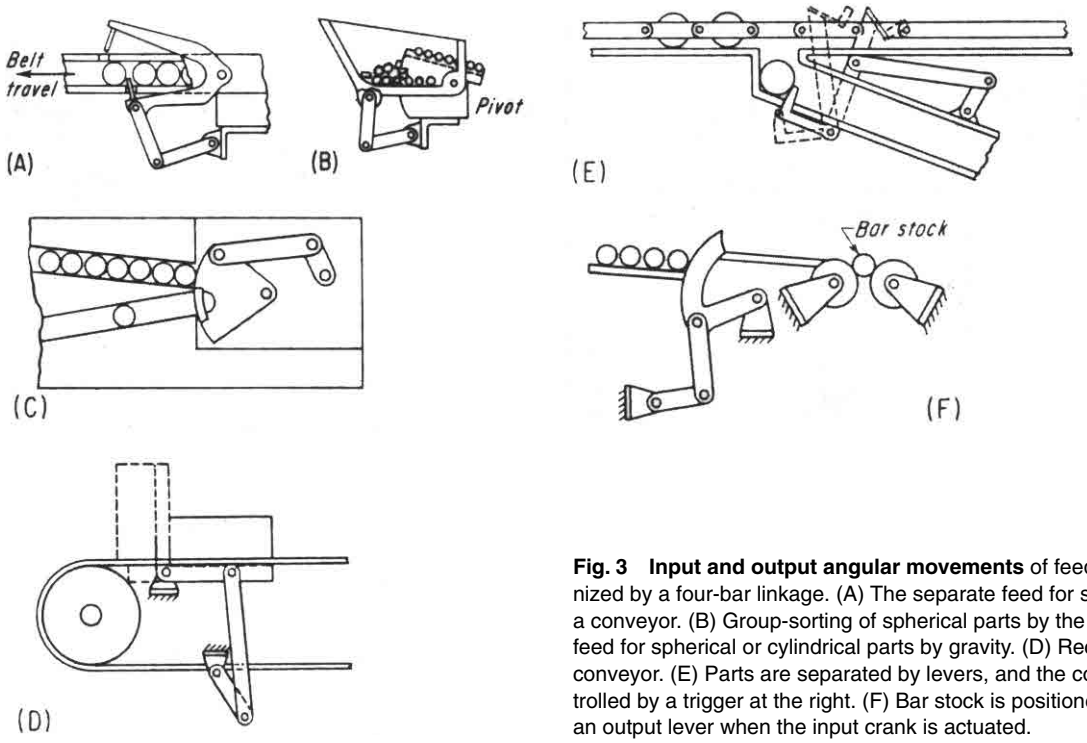

Fig. 3 Input and output angular movements of feeder mechanisms are synchronized by a four-bar linkage. (A) The separate feed for spherical or cylindrical parts on a conveyor. (B) Group-sorting of spherical parts by the tilting hopper. (C) A separate feed for spherical or cylindrical parts by gravity. (D) Rectangular parts are turned on a conveyor. (E) Parts are separated by levers, and the conveyor movement is controlled by a trigger at the right. (F) Bar stock is positioned by the angular oscillation of an output lever when the input crank is actuated.

FEEDER MECHANISMS FOR CURVILINEAR MOTIONS

Four-bar linkages can be combined into six, eight, or more linkages for the feeder mechanisms in cameras, automatic lathes, farm machinery, and torch-cutting machines.

When feeder mechanisms require complex curvilinear motions, it might be necessary to use compound linkages rather than four links. However, four-bar linkages can be synthesized to produce curvilinear motions of various degrees of complexity, and all possibilities for four-bar linkages should be considered before selecting more complex linkages.

For example, a camera film-advancing mechanism, Fig. 1, has a simple four-bar linage with a coupler point *d*, which generates a curvilinear and straight-line motion *a* resembling a D. Another more complex curvilinear motion, Fig. 2, is also generated by a coupler point *E* of a four-bar linkage, which controls an automatic profile cutter. Four-bar linkages can generate many different curvilinear motions, as in Fig. 3. Here the points of the coupler prongs, g_1, g_2, and g_3 on coupler *b*, and g_4 and g_5 on coupler *e*, are chosen so that their motions result in the desired progressive feeding of straw into a press.

A similar feeding and elevating device is shown in Fig. 4. The rotating device crank *a* moves coupler *b* and swinging lever *c*, which actuates the guiding arm *f* through the link *e*. The bar *h* carries the prone fingers g_1 through g_7. They generate coupler curves a_1 through a_7.

As another practical example, consider the torch-cutting machine in Fig. 5A designed to cut sheet metal along a curvilinear path *a*. Here the points A_0 and B_0 are fixed in the machine, and the lever A_0A_1 has an adjustable length to suit the different curvilinear paths *a* desired.

The length B_1B_1 is also fixed. The challenge is to find the length of the levers A_1B_1 and E_1B_1 in the four-bar linkage to give the desired path *a*, which is to be traced by the coupler point *E* on which the cutting torch is mounted.

The graphical solution for this problem, as shown in Fig. 5B, requires the selection of the points A_1 and E_4 so that the distances A_1E_1 to A_8E_8 are equal and the points E_1 to E_8 lie on the desired coupler curved *a*. In this case, only the points E_4 to E_8 represent the desired profile to be cut. The correct selection of points A_1 and E_1 depends upon making the following triangles congruent:

$$\Delta E_2A_2B_{01} = \Delta E_1A_1B_{02}$$
$$\Delta E_3A_3B_{01} = \Delta E_1A_1B_{03}$$
$$\Delta E_8A_8B_{01} = \Delta E_1A_1B_{08}$$

and so on until $E_8A_8B_{01} = E_1A_1B_{08}$. At the same time, all points A_1 to A_8 must lie on the arc having B_1 as center.

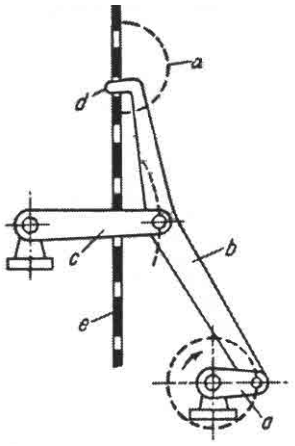

Fig. 1

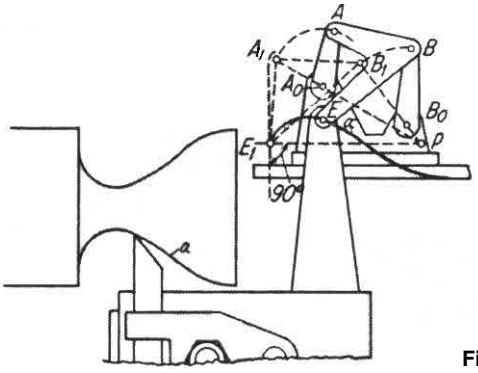

Fig. 2

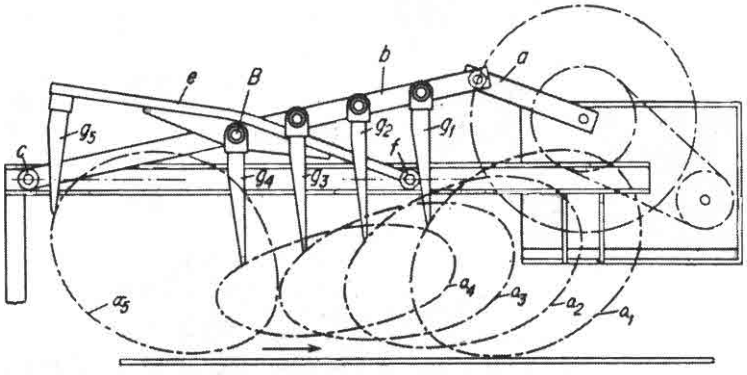

Fig. 3

Fig. 4

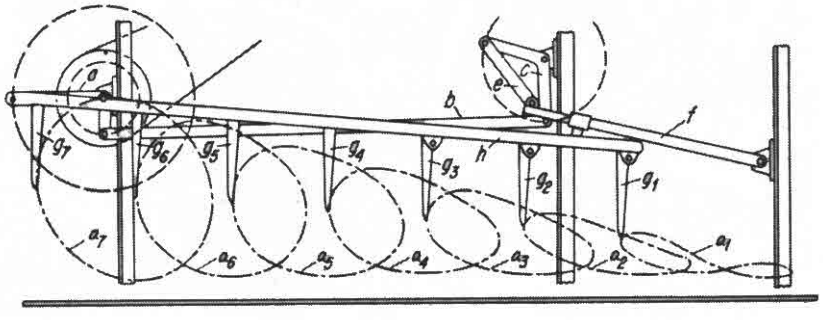

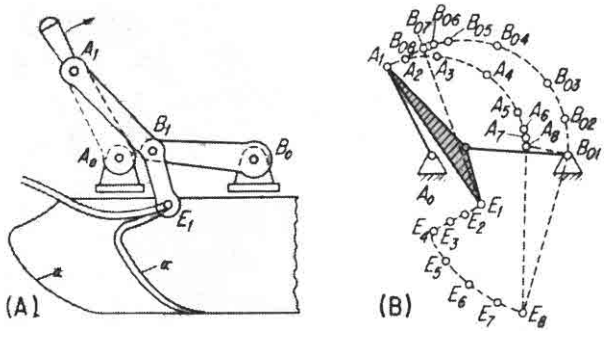

Fig. 5

Synthesis of an Eight-Bar Linkage

Design a linkage with eight precision points, as shown in Fig. 6. In this mechanism the curvilinear motion of one four-bar linkage is coordinated with the angular oscillation of a second four-bar linkage. The first four-bar linkage consists of AA_0BB_0 with coupler point E which generates γ with eight precision points E_1 through E_8 and drives a second four-bar linkage HH_0GG_0. Coupler point F generates curve δ with precision points F_1 through F_8. The coupler points F_2, F_4, F_6, F_8 are coincident because straight links GG_0 and GH are in line with one another in these coupler positions. This is what permits HH_0 to oscillate, despite the continuous motion of the coupler point F. The coupler points F_1 coincident with F_5, and F_3 coincident with F_7, have been chosen so that F_1 is the center of a circle k_1 and F_3 is the center of a circle k_3. These circles are tangent to coupler curve γ at E_1, and E_5, E_3, and E_7, and they indicate the limiting positions of the second four-bar linkage HH_0GG_0.

The limiting angular oscillation of HH_0, which is one of the requirements of this mechanism, is represented by positions H_0H_1 and H_0H_3. It oscillates four times for each revolution of the input crank AA_0, and the positions H_1 to H_8 correspond to input crank positions A_1 to A_8.

The synthesis of a compound linkage with dwell periods and coordinated intermittent motion is shown in Fig. 7. The four-bar linkage AA_0BB_0 generates an approximately triangular curve with coupler point E, which has six precision points E_1 through E_6. A linkage that will do this is not unusual and can be readily proportioned from known methods of four-bar linkage synthesis. However, the linkage incorporates dwell periods that produce coordinated intermittent motion with a second four-bar linkage FF_0HB_0. Here the tangent arcs k_{12}, k_{34} and k_{56} are drawn with EF as the radius from centers F_{12}, F_{34} and F_{56}.

These centers establish the circle with F_0 as the center and pivot point for the second four-bar linkage. Each tangent arc causes a dwell of the link FF_0, while AA_0 rotates continuously. Thus, the link FF_0, with three rest periods in one revolution, can produce intermittent curvilinear motion in the second four-bar linkage FF_0HB_0. In laying out the center, F_0 must be selected so that the angle EFF_0 deviates only slightly from 90° because this will minimize the required torque that is to be applied at E. The length of B_0H can be customized, and the rest periods at H_{34}, H_{12} and H_{56} will correspond to the crank angles ϕ_{34}, ϕ_{12} and ϕ_{56}.

A compound linkage can also produce a 360° oscillating motion with a dwell period, as in Fig. 8. The two four-bar linkages are AA_0BB_0 and BB_0FF_0, and the output coupler curve γ is traversed only through segment E_1, E_2. The oscillating motion is produced by lever HH_0, connected to the coupler point by EH. The fixed point H_0 is located within the loop of the coupler curve γ. The dwell occurs at point H_3, which is the center of circular arc k tangent to the coupler curve γ during the desired dwell period. In this example, the dwell is made to occur in the middle of the 360° oscillation. The coincident positions H_1 and H_2 indicate the limiting positions of the link HH_0, and they correspond to the positions E_1 and E_2 of the coupler point.

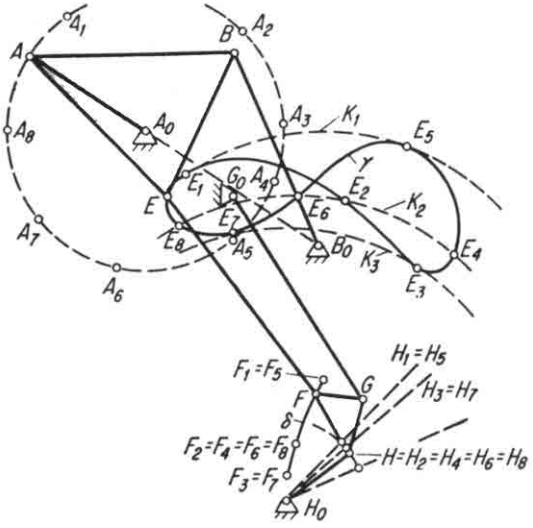

Fig. 6

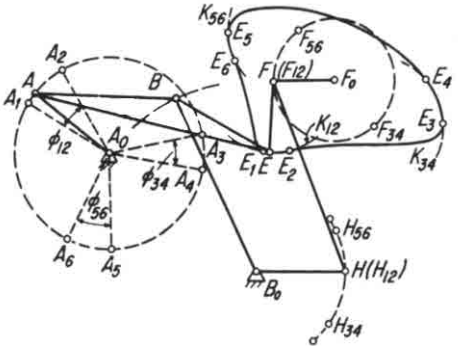

Fig. 7

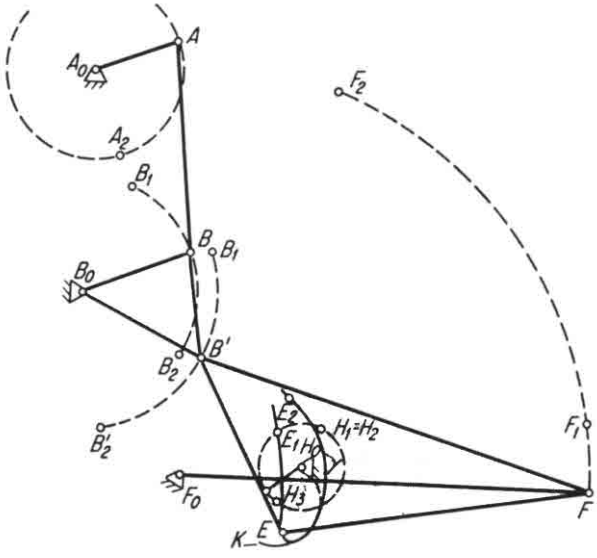

Fig. 8

ROBERTS' LAW HELPS TO FIND ALTERNATE FOUR-BAR LINKAGES

The three linkage examples

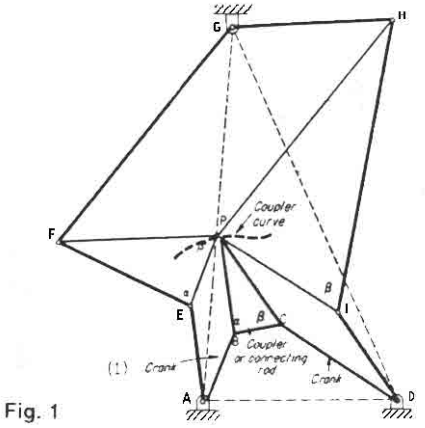

Fig. 1

When a four-bar linkage has been designed or selected from a catalog to produce a desired coupler curve, it is often found that one of the pivot points is inconveniently located or that the transmission angles are not suitable. (A coupler curve is produced by a point on the connecting rod joining the two cranks of the four-bar linkage). According to *Roberts' Law* there are at least two other four-bar linkages that will generate the same coupler curve. One of these linkages might be more suitable for the application.

Robert's Law states that the two alternate linkages are related to the first by a series of similar triangles. This leads to graphical solutions; three examples are shown. The first involves similar triangles, the second is a more convenient step-by-step method, and the third illustrates the solution of a special case where the coupler point lies along the connecting rod.

Method of Similar Triangles

Four-bar linkage *ABCD* in Fig. 1 uses point *P*, which is actually an extension of the connecting rod *BC*, to produce desired curve. Point *E* is found by constructing *EP* parallel to *AB*, and *EA* parallel to *PB*. Then triangle *EFP* is constructed similar to triangle *BPC*. This calls for laying out angles α and β.

Point *H* is found in a similar way, and point *G* is located by drawing *GH* parallel to *FP* and *GF* parallel to *HP*.

The two alternate linkages to *ABCD* are *GFEA* and *GHID*. All use point *P* to produce the desired curve, and given any one of the three, the other two can be determined.

The Step-by-Step Method

With the similar-triangle method just described, slight errors in constructing the proper angles lead to large errors in link dimensions. The construction of angles can be avoided by laying off the link lengths along a straight line.

Thus, linkage *ABCD* in Fig. 2 is laid off as a straight line from *A* to *D*in Fig. 3. Included in the transfers is point *P*. Points *EFGHI* are quickly found by either extending the original lines or constructing parallel lines. Fig. 3, which now has all the correct dimensions of all the links, is placed under a sheet of tracing paper and, with the aid of a compass, links *AB* and *CD* are rotated (see Fig. 4) so that linkage *ABCD* is identical to that in Fig. 2. Links *PEF* and *PHI* are rotated parallel to *AB* and *CD*, respectively. Completion of the parallelogram gives the two alternate linkages, *AEFG* and *GHID*.

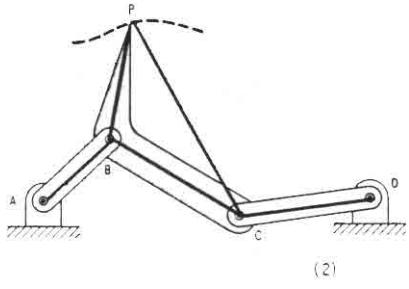

Fig. 2

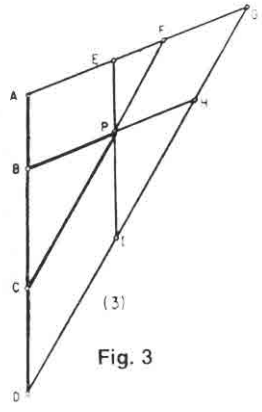

Fig. 3

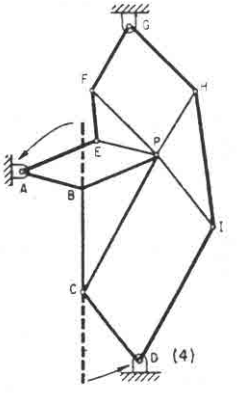

Fig. 4

Fig. 3

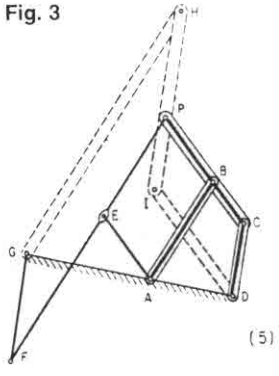

Fig. 1 The method of similar triangles.

Fig. 2, 3, 4 A step-by-step method.

Fig. 5 This special case shows the simplicity of applying Roberts' Law.

Special Case

It is not uncommon for the coupler point *P* to lie on a line through *BC*, as in Fig. 5. Links *EA*, *EP* and *ID* can be found quickly by constructing the appropriate parallel lines. Point *G* is located by using the proportion: *CB*:*BP* = *DA*:*AG*. Points *H* and *F* are then located by drawing lines parallel to *AB* and *CD*.

RATCHET LAYOUT ANALYZED

The ratchet wheel is widely used in machinery, mainly to transmit intermittent motion or to allow shaft rotation in one direction only. Ratchet-wheel teeth can be either on the perimeter of a disk or on the inner edge of a ring.

The pawl, which engages the ratchet teeth, is a beam pivoted at one end; the other end is shaped to fit the ratchet-tooth flank. Usually, a spring or counterweight maintains constant contact between wheel and pawl.

It is desirable, in most designs, to keep the spring force low. It should be just large enough to overcome the separation forces—inertia, weight, and pivot friction. Excess spring force should not be considered for engaging the pawl and holding it against the load.

To ensure that the pawl is automatically pulled in and kept in engagement independently of the spring, a properly drawn tooth flank is necessary.

The requirement for self-engagement is:

$$Pc + M > \mu Pb + P\sqrt{(1+\mu^2)}\mu_1 r_1$$

Neglecting weight and pivot friction:

$$Pc > \mu Pb$$

but $c/b = r/a = \tan \phi$, and because $\tan \phi$ is approximately equal to $\sin \phi$:

$$c/b = r/R$$

Substituting in term (1)

$$rR > \mu$$

For steel on steel, dry, $\mu = 0.15$ Therefore, using

$$r/R = 0.20 \text{ to } 0.25$$

the margin of safety is large; the pawl will slide into engagement easily. For internal teeth with ϕ of 30°, c/b is tan 30° or 0.577, which is larger than μ, and the teeth are therefore self-engaging.

When laying out the ratchet wheel and pawl, locate points O, A and O_1 on the same circle. AO and AO_1 will then be perpendicular to one another; this will ensure that the smallest forces are acting on the system.

Ratchet and pawl dimensions are governed by design sizes and stress. If the tooth, and thus pitch, must be larger than required to be strong enough, a multiple pawl arrangement can be used. The pawls can be arranged so that one of them will engage the ratchet after a rotation of less than the pitch.

A fine feed can be obtained by placing many pawls side by side, with the corresponding ratchet wheels uniformly displaced and interconnected.

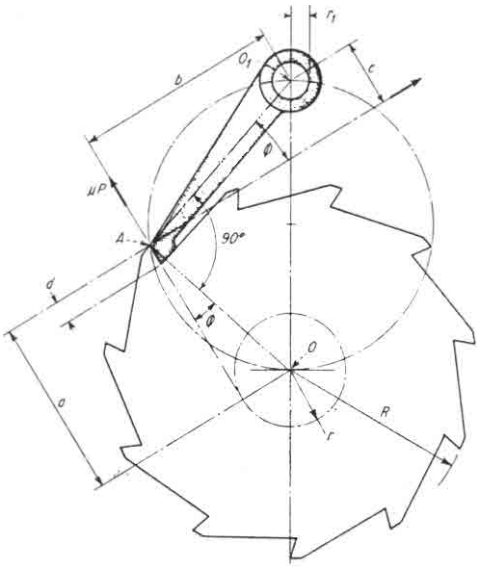

Pawl in compression has tooth pressure P and weight of pawl producing a moment that tends to engage pawl. Friction-force μP and pivot friction tend to oppose pawl engagement.

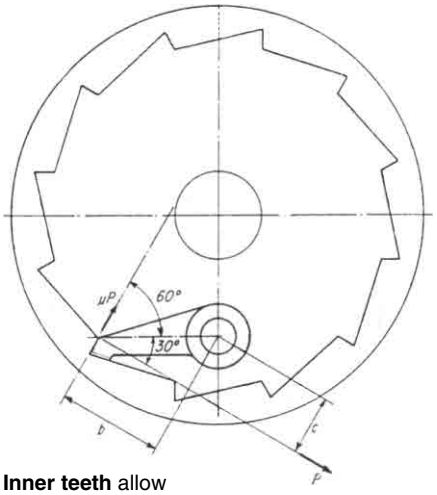

Inner teeth allow compact assembly.

a = moment arm of wheel torque

M = moment about O_1 caused by weight of pawl

$O_1 - O_2$ = ratchet and pawl pivot centers respectively

P = tooth pressure = wheel torque/a

$P\sqrt{(1+\mu^2)}$ = load on pivot pin

μ, μ_1 = friction coefficients

Other symbols as defined in diagrams.

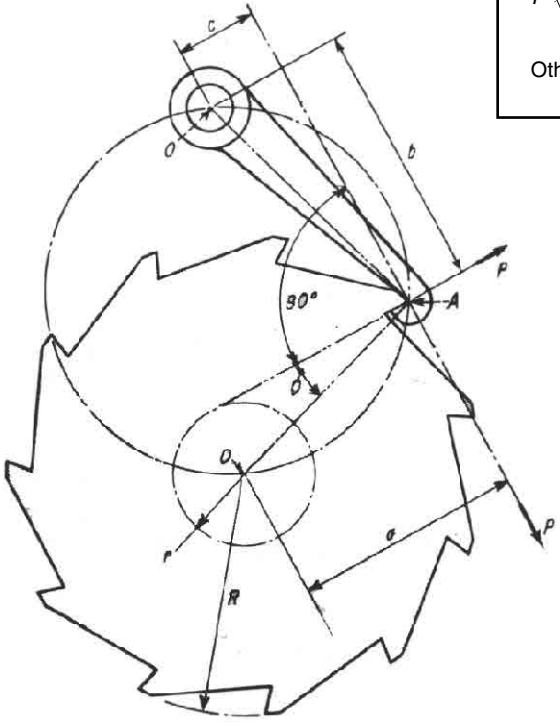

Pawl in tension has the same forces acting on the unit as other arrangements. The same layout principles apply.

SLIDER-CRANK MECHANISM

The slider crank, an efficient mechanism for changing reciprocating motion to rotary motion, is widely used in engines, pumps, automatic machinery, and machine tools.

The equations developed here for finding these factors are in a more simplified form than is generally found in text books.

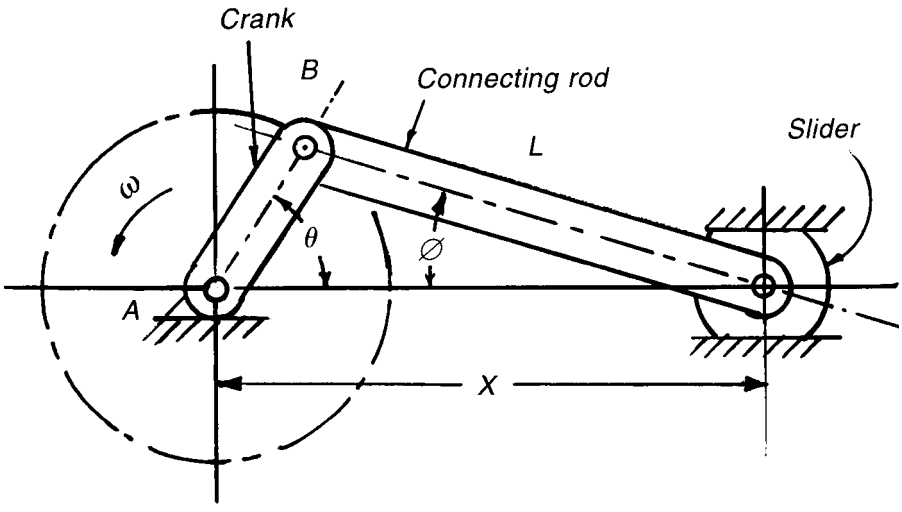

SYMBOLS

L = length of connecting rod

R = crank length; radius of crank circle

x = distance from center of crankshaft A to wrist pin C

x' = slider velocity (linear velocity of point C)

x'' = slider acceleration

θ = crank angle measured from dead center (when slider is fully extended)

ϕ = angular position of connecting rod; $\phi = 0$ when $\theta = 0$

ϕ' = connecting-rod angular velocity = $d\phi/dt$

ϕ'' = connecting-rod angular acceleration = $d^2\phi/dl^2$

ω = constant crank angle velocity

Displacement of slider

$$x = L\cos\phi + R\cos\phi$$

Also:

$$\cos\phi = \left[1 - \left(\frac{R}{L}\right)^2 \sin^2\theta\right]^{1/2}$$

Angular velocity of the connecting rod

$$\phi' = \omega\left[\frac{(R/L)\cos\theta}{[1-(R/L)^2\sin^2\theta]^{1/2}}\right]$$

Linear velocity of the piston

$$\frac{x'}{L} = -\omega\left[1 + \frac{\phi'}{\omega}\right]\left(\frac{R}{L}\right)\sin\theta$$

Angular acceleration of the connecting rod

$$\phi'' = \frac{\omega^2(R/L)\sin\theta[(R/L)^2 - 1]}{[1-(R/L)^2\sin^2\theta]^{3/2}}$$

Slider acceleration

$$\frac{x''}{L} = -\omega^2\left(\frac{R}{L}\right)\left[\cos\theta + \frac{\phi''}{\omega^2}\sin\theta + \frac{\phi'}{\omega}\cos\theta\right]$$